2022

Characterization of Cyclopropyl Synthases Involved in the Maturation of Ribosomally Synthesized and Posttranslationally Modified Peptides

Yi Lien
University of Denver

Characterization of Cyclopropyl Synthases Involved in the Maturation of Ribosomally Synthesized and Posttranslationally Modified Peptides

Abstract

Ribosomally synthesized and post-translationally modified peptides (RiPPs) are a large class of natural products with significant human health implications. RiPPs are synthesized from a genetically encoded precursor peptide that undergoes significant modifications by maturing enzymes, or maturases. Recently, radical-S-adenosylmethionine (rSAM) enzymes have emerged as an important family of RiPP maturases. rSAM enzymes have been shown to install ether, thioether, and carbon-carbon bonds on the precursor peptide. These modifications usually define the backbone structure of the mature RiPP. This thesis describes the characterization of a novel RiPP modification catalyzed by the radical S-adenosylmethionine enzyme TigE. TigE belongs to the TIG biosynthetic gene cluster (BGC), which is encoded by *tigABCDEF*, found in the bacterium *Paramaledivibacter caminithermalis*. The TIG precursor peptide, TigB, is comprised of a repeating TIGSVSG motif. Using a variety of chromatography, mass spectrometry, isotopic labeling, and NMR spectroscopy techniques, we show that TigE catalyzes the formation of C-C bond between the γ-carbons on TigB isoleucine residues (Ile), forming a methyl-cyclopropyl glycine (mCPG). Using crystallography and site-directed mutagenesis, we also revealed that the TigE residue Tyr339 is critical for both the coordination of iron-sulfur clusters and chemistry and could be used as a biomarker for the discovery of other cyclopropyl synthases. This novel RiPP modification provided a reaction scope of radical S-adenosylmethionine enzymes.

Document Type
Thesis

Degree Name
M.S.

Department
Chemistry and Biochemistry

First Advisor
John A. Latham

Second Advisor
Scott Nichols

Third Advisor
Martin Margittai

Keywords
Bioinformatics, Radical-S-adenosylmethionine enzyme, Ribosomally synthesized and posttranslationally modified peptide, Sequence similarity network, TIG biosynthesis

Subject Categories
Biochemistry | Biochemistry, Biophysics, and Structural Biology | Chemistry | Other Chemistry

Publication Statement

Characterization of Cyclopropyl Synthases Involved in the Maturation of Ribosomally

Synthesized and Posttranslationally Modified Peptides.

_____

A Thesis

Presented to

the Faculty of the College of Natural Sciences and Mathematics

University of Denver

_____

In Partial Fulfillment

of the Requirements for the Degree

Master of Science

_____

by

Yi Lien

August 2022

John A. Latham

Author: Yi Lien
Title: Characterization of Cyclopropyl Synthases Involved in the Maturation of Ribosomally Synthesized and Posttranslationally Modified Peptides.
Advisor: John A. Latham
Degree Date: August 2022

ABSTRACT

Ribosomally synthesized and post-translationally modified peptides (RiPPs) are a large class of natural products with significant human health implications. RiPPs are synthesized from a genetically encoded precursor peptide that undergoes significant modifications by maturing enzymes, or maturases. Recently, radical-S-adenosylmethionine (rSAM) enzymes have emerged as an important family of RiPP maturases. rSAM enzymes have been shown to install ether, thioether, and carbon-carbon bonds on the precursor peptide. These modifications usually define the backbone structure of the mature RiPP. This thesis describes the characterization of a novel RiPP modification catalyzed by the radical S-adenosylmethionine enzyme TigE. TigE belongs to the TIG biosynthetic gene cluster (BGC), which is encoded by *tigABCDEF*, found in the bacterium *Paramaledivibacter caminithermalis*. The TIG precursor peptide, TigB, is comprised of a repeating TIGSVSG motif. Using a variety of chromatography, mass spectrometry, isotopic labeling, and NMR spectroscopy techniques, we show that TigE catalyzes the formation of C-C bond between the γ-carbons on TigB isoleucine residues (Ile), forming a methyl-cyclopropyl glycine (mCPG). Using crystallography and site-directed mutagenesis, we also revealed that the TigE residue Tyr339 is critical for both the coordination of iron-sulfur clusters and chemistry and could be used as a biomarker for the discovery of other cyclopropyl synthases. This novel RiPP modification provided a reaction scope of radical S-adenosylmethionine enzymes.

TABLE OF CONTENTS

LIST OF FIGURES

LIST OF TABLES

CHAPTER ONE: INTRODUCTION

RiPP Biosynthesis

Ribosomally synthesized and post-translationally modified peptides (RiPPs) are a large and diverse family of natural products.[1] They serve important critical physiological roles functions in the host species.[2–4] For example, some RiPP products were found to be quorum sensing molecules,[5–7] antimicrobials,[8] and redox cofactors.[9,10] Importantly, RiPPs have gained attention as a potential source of biologically pharmacophores, such as antibiotics and anticancer agents[11] because of their immense distribution in bacteria and their potential to be engineered.[12,13] RiPPs could be a resource for antimicrobial resistance crisis since several of them have been found to inhibit the growth of pathogenic bacteria. Currently, three major classes of RiPP - lasso peptides, cyclotides, and lanthipeptides - have been shown to display antimicrobial activity against Gram-negative bacteria due to their specific post-translational modifications (PTMs).[14,15] The most notable is nisin, a lanthipeptide from *Lactococcus lactis*, which has been applied to food preservation for several decades.[16] Various lasso peptides are active against both Gram-negative and Gram-positive bacteria. For instance, MccJ25 exhibits antibacterial activity against Gram-positive bacteria, such as, *Salmonella*, *Shigella flexneri*, *E. coli*, and *Enterobacter bugandensis*.[17,18] Sviceucin was found to be active against Gram-positive bacteria, including *Bacillus megaterium*, *Lactobacillus bulgaricus*, *Staphylococcus aureus*, and

1

Lactobacillus sakei.[19] Lastly, cyclotides were examined to possess weak antibacterial activity by disrupting the cell membrane.[20] However, including the examples mentioned above, none of the antimicrobial RiPPs were currently approved for clinical use in humans because of their poor solubility and bioavailability. Furthermore, RiPPs could be a resource for the ongoing antimicrobial resistance crisis. For instance, many RiPP antibiotics have been found to inhibit the growth of multidrug resistant bacteria. Specifically the RiPPs patellamides B, C, and D have been reported to reverse multidrug resistance in *Prochloron didemni*.[21,22] Despite the potential for RiPPs to impact human health, it remains difficult to predict structures directly from biosynthetic gene clusters (BGCs) and to identify new RiPP BGCs that can lead to the discovery of new chemical structures. A reason for this is the field tends to focus on classes of well characterized RiPPs and their modifying enzymes. To address these limitations, an understanding of the chemistry within the PTMs of natural products is important.

To synthesize these functional natural products, RiPP precursor peptides undergo significant PTMs by diverse families of tailoring enzymes, or maturases.[23–25] RiPPs maturation starts from a genetically encoded long and ribosomally synthesized precursor peptide. This peptide typically contains 20-110 amino acid residues in length. After the synthesis of precursor peptide, the maturase enzymes sequentially modify the precursor peptide. Those enzymes are thought cyclases, proteases, transporters. For example, NisB is the nisin dehydratase that catalyzes eight dehydrations on Ser and Thr in the biosynthesis of the antibacterial peptide nisin.[1] YcaO heterocyclases are the most common PTM enzymes in bacteria and archaea and install both thiazoline and oxazoline on Cys, Ser, or Thr residues.[2] MftC is a radical S-adenosylmethionine protein in mycofactocin

2

biosynthesis. It catalyzes the decarboxylation of the C-terminal tyrosine residue on its substrate.[3] In general, following modification of the peptide, a peptidase hydrolyzes the mature product to form the mature RiPP.[26] When we take a closer look at the precursor peptides of RiPPs, most of them have a leader, core, and follower sequence. The leader sequence often dictates the binding of tailoring enzymes. In the case of RiPPs with multiple core peptides, the leader peptides play a significant role in post-translational modification, export, immunity and enzyme recognition.[27] The follower sequence provides a cleavage sign for the protease and is eventually removed during the maturation process to deliver the final natural product. The core region is where the tailoring enzymes install PTMs (Figure 1A).

A notable example of RiPP maturation is pyrroloquinoline quinone (PQQ) biosynthetic pathway. PQQ is a water soluble, heat-stable, redox cofactor. Its unique redox-feature has been reported to utilized by various dehydrogenases, oxidases, oxygenases, hydratases, and decarboxylases due to the high redox potential.[28] The pathway is encoded by six genes, *pqqABCDEF*. PqqA is the precursor peptide that recognized by the recognition element, PqqD.[29] Next, the PqqAD complex is bound by the radical S-adenosylmethionine (rSAM) enzyme PqqE, which forms a C-C bond between Glu and Tyr on the precursor peptide. Subsequently, the protease PqqF, hydrolyzes the Glu-Tyr crosslink from the precursor peptide. The Glu-Tyr dimer is then oxidized and cyclized by the oxidases PqqB and PqqC, yielding PQQ (Figure 1B).

A
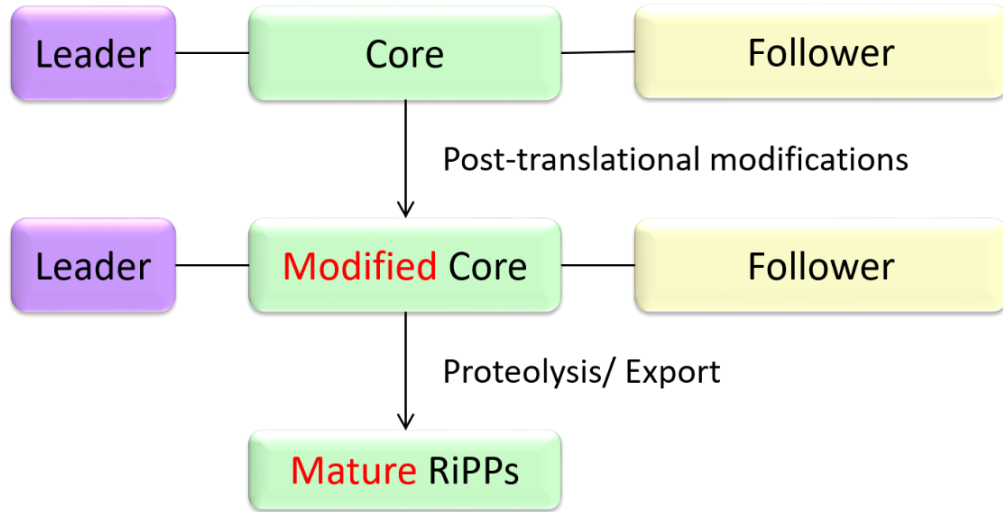
B
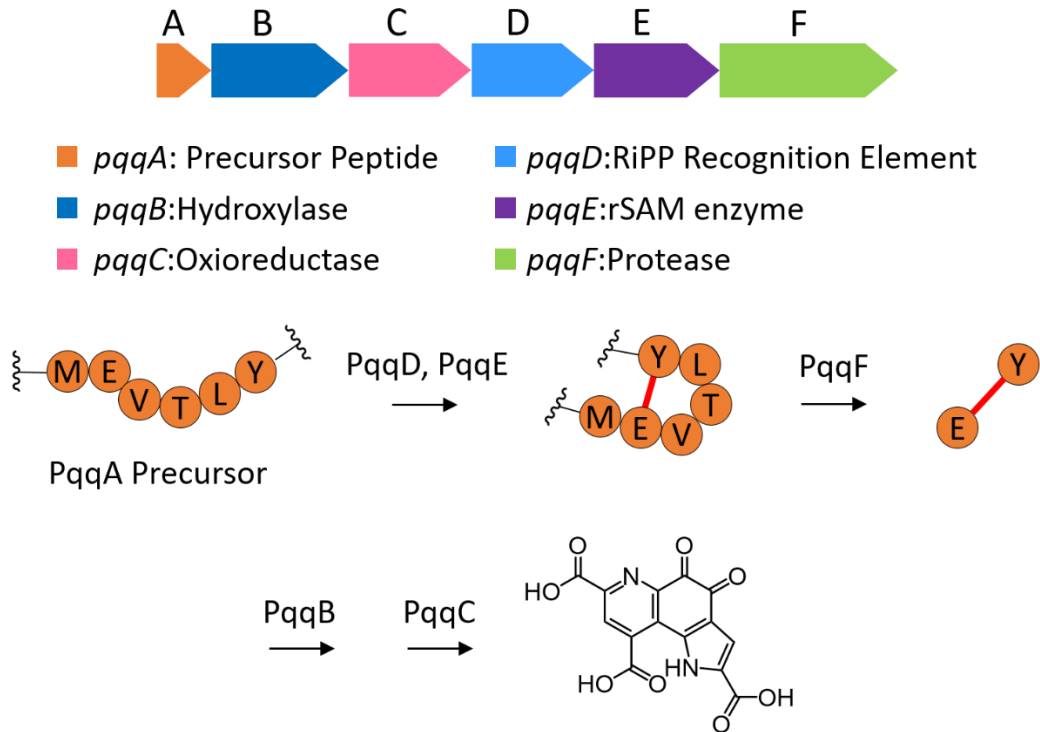
Figure 1. A cartoon depiction of RiPP biosynthesis A) Generic representation of precursor peptide. B) Pyrroloquinoline quinone biosynthesis pathway presenting how a precursor peptide is modified by gene-encoded enzymes within the cluster, resulting in a mature natural product.

Discovery of the RiPP Biosynthetic Pathways

Before 2006, user-friendly genome mining tools for RiPP discovery did not exist. Instead, researchers used a BLAST analysis[30] to search genome based on certain PTM enzymes.[31,32] In 2006, the first web tool was developed by Jong et al. spelling as BAGEL.[33] BAGEL performs a rule-based strategy, where it implements six-frame translation of genomic region, which is used to search for the motifs and core peptides and classifies them into the RiPPs class.[34,35] The core peptide is detected by homology to the already known core peptides or the expected properties of the given class.[34] In 2011, an integrated genome mining tool antiSMASH was designed to find different biosynthetic gene cluster (BGS) including RiPPs. Later, the web tool, Rapid ORF Description and Evaluation Online RODEO, was designed to analyze RiPPs. RODEO implements profile hidden Markov models (HMM)-based local genomic analysis and precursor peptide/structure prediction by implementing heuristic scoring, motif analysis, and machine learning to detect RiPPs.[36] Notably, the sactipeptide RiPP biosynthetic gene cluster was mapped via the rSAM-SPASM enzymes, which catalyze the sactionine bond by employing the recent improved version of RODEO 2.0.[37] Recently, bioinformatics web tools that participate in the RiPPs classification and cluster mining were divided into four groups[35]: 1) Searching for conserved RiPP tailoring enzymes 2) Searching for PTM enzymes and precursor peptides 3) Searching by using machine learning 4) BGC comparison and clustering by sequence similarity networks (SSN) (Table2).

Searching both PTM enzymes and precursors			
Method	**Description**	**Year**	**References**
BAGEL3	Combines direct mining for the gene and indirect mining via context genes.	2013	38
RODEO	Rapid ORF Description and Evaluation Online: Analyzes RiPP BGCs via heuristic scoring, motif analysis, and machine learning	2017	36
BAGEL4	Adds more features to BAGEL3, including the integration of RNA-Seq data, an improved web blast and integration of promoter and terminator predictions.	2018	34
RODEO2	Launched with support of more RiPPs classes.	2019	39
BGCs comparison and clustering by similarity network			
EFI-EST	Enzyme Function Initiative-Enzyme Similarity Tool: The tool can create SSNs for the closest neighbors.	2015	40
BiG-SCAPE	Biosynthetic Gene Similarity Clustering And Prospecting Engine: facilitates fast and interactive sequence similarity network analysis of BGS and gene cluster families	2020	41
Searching conserved RiPP tailoring enzymes			
antiSMASH 2.0	Analyzes draft genomes comprising multiple contigs and detects additional classes of secondary metabolites, such as oligosaccharide antibiotics.	2013	42
PRISM	PRediction Informatics for Secondary Metabolomes: First launched as a genome mining tool that link BGCs with natural products.	2015	43
RiPP- PRISM	Provides the systematic investigation of RiPP genetic and chemical space and targets the discovery of RiPPs based on genome sequencing.	2016	44
PRISM3	Increases the cluster detection and improves sequence input and ORF detection	2017	43
antiSMASH 4.0	Improves the chemistry prediction and gene cluster boundary identification	2017	45
antiSMASH 5.0	Updates the secondary metabolite genome mining.	2019	46

Mining precursor peptides using machine learning			
RiPPMiner	Classify the precursor into nine sub-classes of RiPPs by support vector machines.	2017	[47]
DeepRiPP	Integrates multiomics data to automate discovery of novel RiPPs.	2019	[48]

Table 1. Genome mining strategies of RiPPs.

It has been 15 years since the first RiPP mining tool was designed. Since, different bioinformatic strategies have been applied to RiPP mining, such as targeting conserved tailoring enzymes or targeting the precursor peptide in their search. These mining tools are useful and commonly used in RiPP research which can effectively isolate the molecules shared with gene similarity. However, these studies do not expand the scope of chemical modifications which impedes the discovery of new RiPPs.

Radical SAM Enzymes with a SPASM Domain

The radical S-adenosylmethionine (rSAM) superfamily has become increasingly common in RiPP maturation[49]. rSAM enzymes participate in RiPP maturation by utilizing a [4Fe–4S] cluster and SAM to initiate a diverse set of radical reactions, in most cases via the generation of a 5'-deoxyadenosyl radical (5'-dA•) intermediate.[50] The 5'-dA• abstracts a hydrogen atom from the substrate and produces a substrate radical. The radical on the substrate drives the PTM, resulting in the mature RiPP (Figure 2A). To initiate the reductive cleavage of SAM, a [4Fe-4S] cluster needs to be reduced from +2 oxidation state to the +1 oxidation state. In vitro, the widely-used reducing agent are biological reducing system Fpr/Fld and chemical reductants such as dithionite. The NADPH-dependent flavodoxin reductase system was found to be able to transfer the electron from NADPH to

the [4Fe-4S] cluster. The oxidation of NADPH to $NADP^+$ generates two electrons which are used to reduce flavin adenine dinucleotide (FAD) bond by flavodoxin reductase (Fpr). Next, the reduced Fpr passes the electrons to a second FAD bound by flavodoxin (Fld). Lastly, one electron is passed to the rSAM [4Fe-4S] cluster, reducing it from +2 to +1 oxidation state (Figure 2B).[51] The reduced [4Fe-4S] cluster then has the ability to transfer the radical to SAM and generate the 5'-dA• by rSAM enzymes.

A
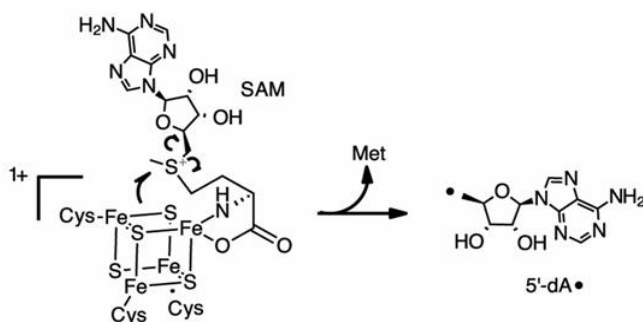
B
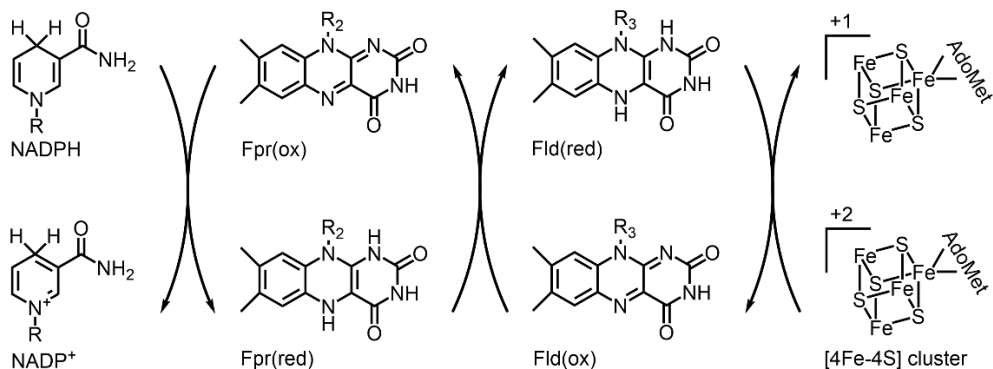
Figure 2. Strategy of SAM cleavage. A) Schematic representation of the homolytic cleavage of SAM enzyme, yielding the 5'-deoxyadenosyl radical (5'-dA•) B) NADPH-dependent flavodoxin reductase system reduces the AdoMet radical cluster.

Despite the diversity of rSAM enzymes, there are unifying structural and mechanistic themes. The majority of rSAM enzymes involved in RiPP modification can be dissected into two domains, a TIM-Barrel domain and a SPASM domain. The TIM-Barrel domain was named after the partial $(\beta/\alpha)_6$ triose-phosphate isomerase (TIM) barrel fold that

8

maintains the structure of the enzyme. It has a conserved $CX_3CX\varphi C$ motif (where φ is an aromatic residue) that typically binds the [4Fe–4S] cluster. In 2011, Haft and Basu[52,53] recognized that enzymes with the rSAM motif appear to be colocalized with putative peptide modifying pathways. They observed that in addition to the main cluster, the putative peptide modifying rSAM members have the C-terminal extension called "SPASM," named after the founding members <u>s</u>ubtilosin A, <u>p</u>yrroloquinoline quinone, <u>a</u>naerobic <u>s</u>ulfatase, and <u>m</u>ycofactocin.[54] The X-ray crystal structure of anaerobic sulfatase-maturating enzyme (anSME) from *Clostridium perfringens* corroborated the observations by Haft and Basu. Indeed, the SPASM domain on AnSME was found to coordinate two auxiliary [4Fe-4S] clusters, in addition to the rSAM [4Fe-4S] cluster. It should be noted that although AnSME is not a RiPP maturase, its structure is homologous to RiPP-modifying rSAM-SPASM enzymes (Figure 3A).
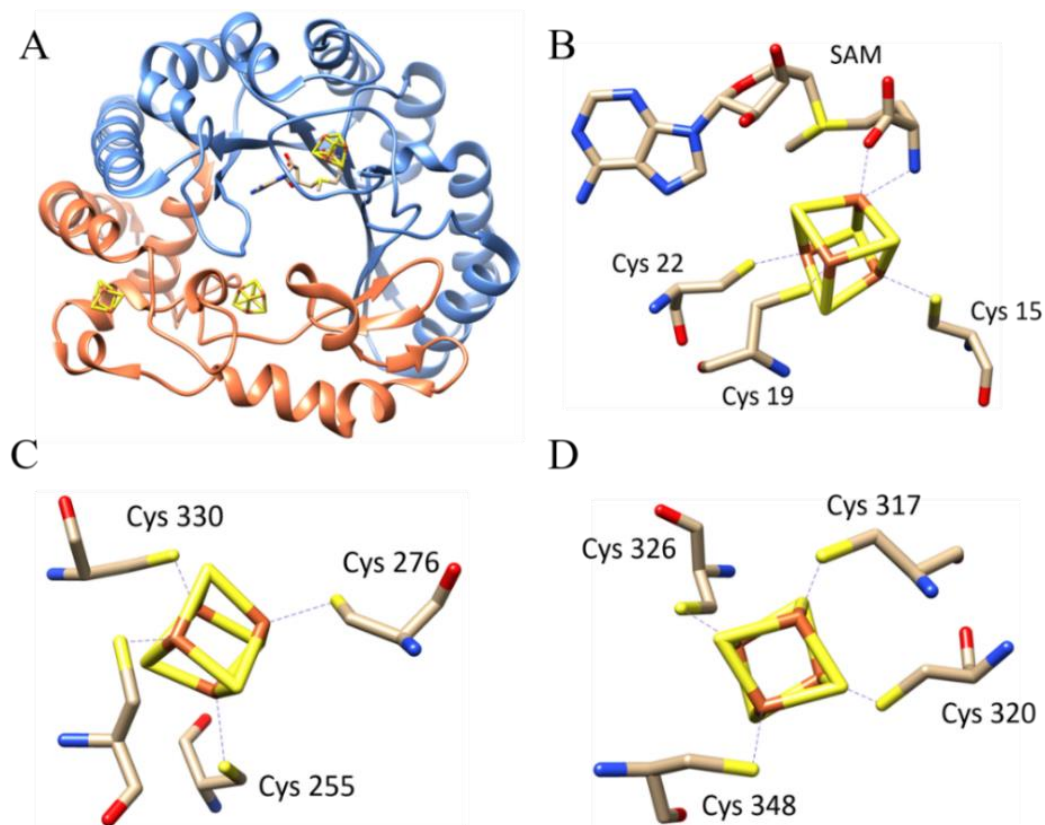
Figure 3. A cartoon depiction of the rSAM-SPASM protein AnSME. A) Crystal structure of radical SAM enzyme anSME. (PDB ID: 4K35) Radical SAM TIM-barrel domain is colored blue, SPASM domain is in coral. Within the iron-sulfur cluster, the Fe atoms are colored red, and the sulfur atoms are colored yellow. The SAM molecule is represented in stick mode. B) rSAM [4Fe–4S] cluster. C) AnSME auxiliary [4Fe-4S] cluster I. D) AnSME auxiliary [4Fe-4S] cluster II.

As mentioned above, AnSME binds three [4Fe-4S] clusters. The rSAM [4Fe–4S] cluster is located in a loop following the β1 strand in the parallel $(\beta/\alpha)_6$ partial triose phosphate isomerase (TIM) barrel. The amino acid residues C15, C19, and C22, which belong to the $CX_3CX\varphi C$ motif, each ligate an iron atom of rSAM [4Fe–4S] cluster (Figure 3B). Two additional auxiliary [4Fe-4S] clusters of AnSME were found in the SPASM domain. Residues C255, C261 and C276 coordinate the first auxiliary cluster (Figure 3C) while residues C317, C320, and C326 coordinate the second auxiliary cluster (Figure 3D).

This structure shares homology with rSAM enzymes and has been applied to bioinformatics RiPP mining tools.

Auxiliary clusters are believed to serve dual roles as both an electron acceptor and/or electron donor depending on the reaction.[55] The auxiliary clusters in MftC help to catalyze two distinct reactions, oxidative and redox-neutral, on the precursor peptide.[56] It has been proposed that both rSAM [4Fe–4S] cluster and two auxiliary [4Fe–4S] clusters are required for MftA modification. First haft e$^-$ acceptor and the second haft e$^-$ donor.

rSAM enzymes catalyze a variety of PTMs on the precursor peptide. They include the formation of C-C bonds[7,57,58], C-S bonds[37,59–63], C-O bonds[64], epimerization[65,66] and methyltransfer.[67–70] The first reported *in vitro* C−C bond formation by a rSAM-SPASM in RiPP biosynthesis involved streptide.[7,71] Streptide is a quorum sensing molecule that is synthesized from the precursor peptide, StrA, by the *str* gene cluster.[72] Within the cluster, the rSAMS-PASM protein, StrB, was shown to install a C_β-C7 bond between Lys and Trp, yielding a cyclophane.[7,73] Soon after, a PqqE was reported to catalyze the formation of a C$_\gamma$-C3 bond between Glu and Tyr on the precursor peptide PqqA, a critical step in the formation of PQQ. [57] More recently, XyeB, GrrB, FxsB, WgkB, and RrrB have all been reported to catalyze the formation of cyclophanes on their respective precursor peptide.[74–77] The linkages from nonaromatic carbons can occur from C_α, C_β, C_γ, or C_δ and typically are attached to the C3 of Tyr or, less discriminately, to C4-C8 of Trp. From these studies, it is becoming more apparent that rSAM-SPASM proteins have been recruited to install cyclophanes in RiPP biosynthesis.

The first thioether bond between C_α and S was discovered by the studies on AlbA. They were later classified as sactipeptide[78] (sulfur-to-alpha carbon thioether cross-linked

peptides) and include sporulation killing factor (SKF),[79] the thuricin family,[80,81] ruminococcin C,[82] six-cysteines-in-forty-five (SCIFF),[83] and streptosactin.[84] SkfB catalyzed the formation of a thioether bond between a C_α-S bond on the precursor peptide to (SKF)[79] and on ThnB, showing that it installed a C_α-S bond on the precursor peptide of thuricin H. While reports of C_α-S thioether bridges were predominant in the early stages of rSAM dependent RiPP discovery, it should be noted that C_β-S and C_γ-S bonds, or ranthipeptides (radical non-α-thioether peptides), have since become increasingly common. The first rSAM-SPASM enzyme to catalyze non-C_α-S thioether bonds was QhpD.[85] QhpD installs both C_β-S and C_γ-S thioether bonds during the maturation of the γ-subunit (QhpC) of quinohemoprotein amine dehydrogenase.[85]

Lastly, rSAM-SPASM proteins have been shown to install C-O bonds on RiPP precursor peptides. Recently, the Seyedsayamdost group reported on the formation of an aliphatic ether in a streptococcal quorum sensing molecule encoded by the *tqq* biosynthetic gene cluster.[64] TqqB was shown to catalyze the formation of a C-O bond between a Thr-derived alcohol and the C_α of an adjacent Gln on the precursor peptide TqqA (Table 1).[64]

Bond formation	Current List of Known rSAM-SPASM Proteins
C-C Bond	PqqE[57,86], StrB/SuiB[7,73], MftC[87–89], RrrB[90], WgkB[76], XyeB[75,91], GrrB[75,91], FxsB[75,91], TvgB[92]
C-S Bond	AlbA[93,94], CteB, Tte1186[95,96], ThnB[62], QhpD[97], RumC[82], QmpB[98], NxxcB[99], GggB[84], PapB[100,101]
C-O Bond	TqqB (Twitch)[102]
Other	PlpD[103]

Table 2. Current list of known rSAM-SPASM proteins.

We now know that rSAM-SPASM enzymes are widely used peptide-modifying enzymes, with expanding functionality. The development of new bioinformatic tools has led to genome-based discovery of rSAM-dependent RiPPs and has been successfully employed in the discovery of sactipeptides,[82] ranthipeptides,[8] and ryptides,[77] to name a few. Despite the progress of mining tools and the growing interest of rSAM-dependent RiPP natural products, little of the full extent of modifications is known. The variety of different modifications, the rules that these rSAM enzymes follow, the mechanism that makes these enzymes selectively target the precursor peptides, and the relation between the activities and the structure need to be answered. Therefore, we sought to expand the number of RiPP biosynthetic pathways that require rSAM enzymes to further understand the chemistry of this field.

Identification of the TVG Biosynthetic Pathway

Recently, our lab leveraged rSAM enzymes belonging to the rSAM-SPASM (IPR023867) subfamily,[54] in a bioinformatic search to discover new chemistry and new RiPP modifications (Figure 4A and 4B).[92] In particular, the IPR023867 rSAM subfamily consists of 24,000 protein sequences (at the time of analysis) including many rSAM enzymes that are known[104] or expected[63] to modify peptides. As mentioned above, members of the rSAM-SPASM subfamily are known RiPP modifying enzymes and the majority have been shown to install critical bonds that define the skeleton of the mature RiPP.[105] Our bioinformatic analysis identified a substantial number of potentially new RiPP classes that were previously unannotated or unexplored. From this analysis, we targeted a RiPP biosynthetic gene cluster (BGC) that encoded a precursor peptide with a

13

repeating TVGG motif and a single rSAM-SPASM enzyme, TvgB (Figure 4C). We structurally characterized the TvgB reaction product and showed that TvgB installs repeated units of cyclopropylglycine (CPG), where a new bond is formed between the Cγ carbons on the precursor Val (Figure 4D). From this work, we discovered the first rSAM enzyme to catalyze the formation of a cyclopropane motif without being coupled to methyl addition and the first rSAM enzyme to catalyze the formation of a CPG in RiPP maturation. Since cyclic peptide natural products play important roles as therapeutics. Enzymatic or chemical macrocyclization is the key transformation for constructing these drug molecules. Methods to generate new and diverse cyclic peptides are essential leading to predictable synthesis of nature products derived peptides in the fields of pharmaceutical chemistry and chemical biology. [106] We set out to determine the extent of the TvgB family of rSAM enzymes.

The overall goal of this thesis was to determine the extent of CPG forming rSAM enzymes. To do so, we bioinformatically annotated and expanded the family of cyclopropyl (CP) synthases associated with RiPP biosynthesis. We used this analysis to discover an unprecedented methyl-CPG containing RiPP. We demonstrated *in vitro,* that the CP synthase annotated as TigE, catalyzes the formation of methyl-CPG from Ile residues within a TIGSVS repeating sequence on the precursor peptide. To gain insight to how TigE catalyzes its reaction and recognizes substrates, we solved the crystal structure of the protein. In doing so, we discovered an unusual [4Fe-4S] amino acid ligand which we propose could be used as a biomarker to discover other CP synthases or other rSAM enzymes that catalyze new chemistries.
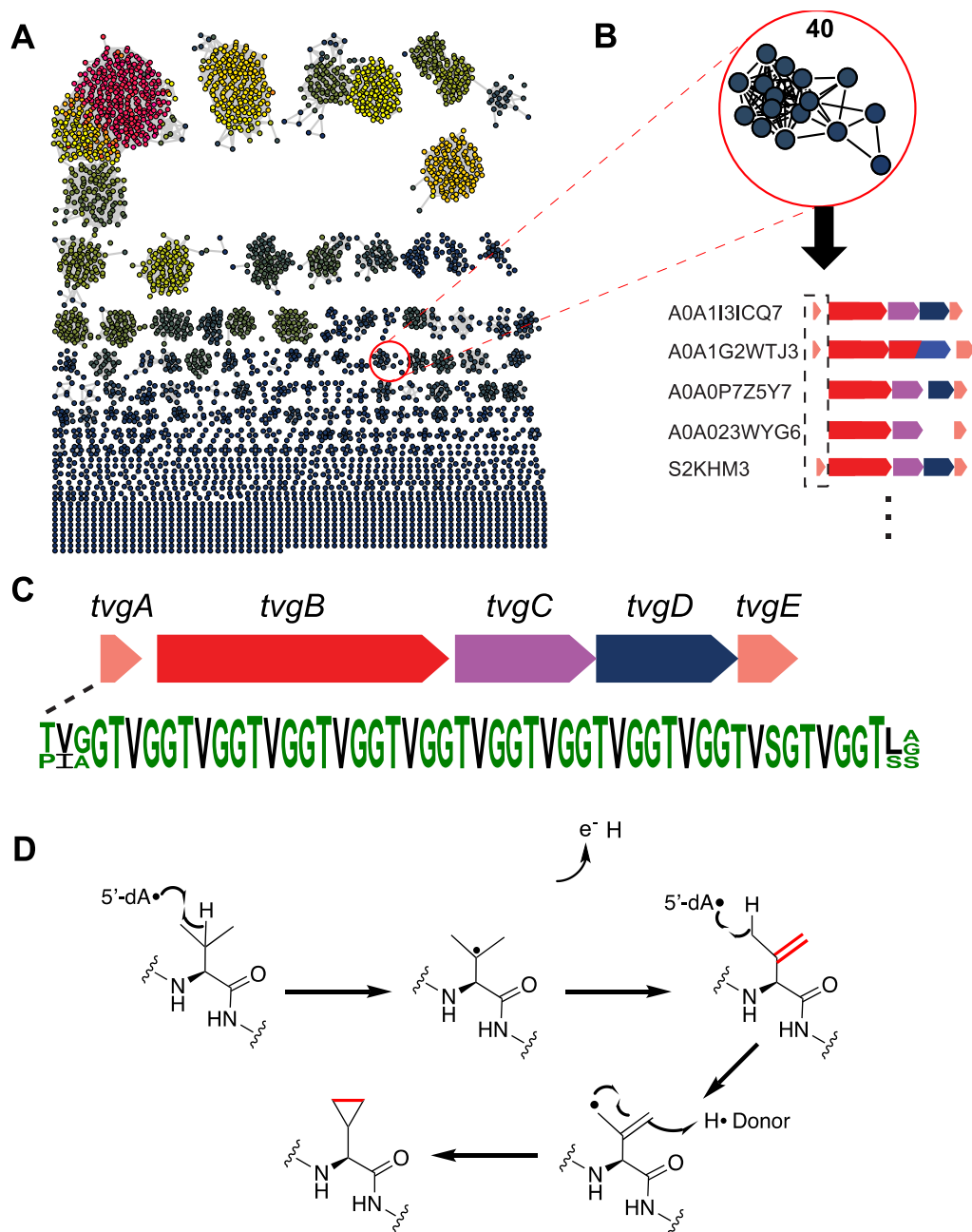
Figure 4. A bioinformatic workflow for rSAM enzymes. A) The sequence similarity network of the IPR023867 family of rSAM enzymes using the Uniref90 database, an E value of 10-80, and a 40% sequence identified cutoff. Clusters were colored by gene description. B) The representative sequence for each cluster was used to generate a genome neighborhood diagram from which precursor peptides were identified and used in subsequent sequence alignments. rSAM, radical-SAM. C) A depiction of the TVG biosynthetic pathway. D) A schematic representation of the proposed mechanisms for TvgB.

CHAPTER TWO: MATERIALS AND METHODS

Bioinformatic Analysis of IPR023867

The Radical-SAM.org webtool was used to search for protein networks comprised of TvgB homologues.[106] The sequence similarity network (SSN) cluster (1-1-201:AS65) that defined TvgB as well as 49 other Uniprot IDs was identified. Using the Genome Neighborhood Diagram tool, all available precursor peptides in the intergenic regions were identified and the conserved repeating regions of the peptide sequences were mapped to each TvgB homologue. The SSN was then reorganized by peptide sequence to yield the network.

Preparation of TigE

SAMN02745912_03532 gene (UniProt: A0A1M6T2I7) that encoded by *Paramaledivibacter caminithermalis* str. DSM 15212 was synthesized and cloned into the pET-28a vector (Genscript) by using NdeI and XhoI as the restriction sites. The pPH151 plasmid, which contains the *suf* operon and sequence-verified */pET28a* plasmid was co-transformed into *E. coli* BL21 (DE3). A single colony was picked and incubated starting from 10 mL of terrific broth and subjected to the 6 L large-scale incubation. The cultures were grown and shook under 37 °C at 200 rpm until the $OD_{600\,nm}$ reached 0.9. After cooling down in the 4 °C cold room, 1 mM isopropyl thiogalactopyranoside, 1.5 g/L of sodium fumarate, and 1X auto-induction metals were added to the media for induction. The

16

induction process was conducted at 21 °C for 12 h. to 16 h. The cells were harvested by centrifuging at 7,000 rpm for 10 min. The purification and protein reconstitution were performed in the anaerobic environment. The collected cell pellet was re-suspended in the degassed lysis buffer (50 mM HEPES, 300 mM NaCl, pH 8.0) with 1% w/v 3-[(3-cholamidopropyl) dimethylammonio]-1-propanesulfonate (CHAPS), 0.1 mg/g of lysozyme, and 0.1 mg/g DNase. After sonication, the lysate was centrifuged at 14,000 rpm for 10 min at 4 °C. The protein was purified from the soluble supernatant by Ni^{2+}-affinity chromatography. A 5 mL HisTrap HP column was washed and prepared with lysis buffer. TigE bound on the column and was eluted with elution buffer (50 mM HEPES, 300 mM NaCl, 100 mM Imidazole, pH 8.0). Using a desalting column, purified TigE was exchanged into the storage buffer (50 mM HEPES, 300 mM NaCl, 10 mM DTT, 10% glycerol, pH 8.0).

Protein Reconstitution

To reconstitute TigE, 10 mM DTT, and 12 molar equivalents of both $FeCl_3$ and Na_2S were added to the protein solution and stirred on ice for 30 min. The reconstitution solution was centrifuged at 7,000 rpm for 10 min. Precipitation in the supernatant was removed through the 0.2 um sterile membrane filter. The buffer of reconstituted protein was exchanged to the storage buffer and concentrated by a 50 kDa concentrator (MilliporeSigma). The protein was stored at -80 °C for further use.

Flavodoxin and Flavodoxin Reductase Purification

Flavodoxin and flavodoxin reductase were cloned from *E. coli* into sequence-verified *pET11a* and *pET24b* plasmids respectively. The plasmid was transformed into *E. coli* BL21 (DE3) to optimize the expression of the target protein. A single colony was picked and incubated starting from 10 mL of lysogeny broth and subjected to the 1 L large-scale incubation. The cultures were grown and shook under 37 °C at 200 rpm until the $OD_{600 nm}$ reached 0.9. After cooling down in the 4 °C cold room, 1 mM isopropyl thiogalactopyranoside were added to the media for induction. The induction process was conducted at 21 °C for 12 h. to 16 h. The cells were harvested by centrifuging at 7000 rpm for 10 min. The collected cells pellet was re-suspended in the lysis buffer (50 mM HEPES, pH 7.5) with 1% w/v 3-[(3-cholamidopropyl) dimethylammonio]-1-propanesulfonate (CHAPS), 0.1 mg/g of lysozyme, and 0.1 mg/g DNase. After sonication, the lysate was centrifuged at 14,000 rpm for 10 min at 4 °C. The protein was purified from the soluble supernatant aerobically by ion-exchange chromatography. Two connected 5 mL HiTrap DEAE columns were washed and prepared with lysis buffer. Flavodoxin bound on the column and was gradient eluted with elution buffer (50 mM HEPES, 500 mM NaCl, pH 7.5). The gradient program was as follows: 0–100% elution buffer in 30 min at a flow rate of 5.0 mL/min. Using a desalting column, purified TigE was changed into the degassed storage buffer anaerobically (50 mM HEPES, 300 mM NaCl, 10 mM DTT, 10% glycerol, pH 8.0). Protein purity remained at >97% as determined by SDS-PAGE. Flavodoxin concentration was determined by measuring the absorbance at 464 nm (molar extinction coefficient = 8420 $M^{-1}cm^{-1}$) and flavodoxin reductase concentration was measured the absorbance at 456 nm (molar extinction coefficient = 7100 $M^{-1}cm^{-1}$).

EPR Spectroscopy Analysis

The TigE sample with reduced iron-sulfur clusters was achieved by addition of excess (10 mM) dithionite to 250 μL of 300 μM TigE in storage buffer (50 mM HEPES, 300 mM NaCl, 10 % glycerol, 1 mM DTT and pH 8). Samples were transferred into 4 mm outside diameter quartz tubes in the inert atmosphere chamber and flash frozen in liquid nitrogen. The tubes were temporarily capped with clamped tygon tubing, removed from the chamber, partially evacuated, back-filled with a partial pressure of helium (100 mTorr) to facilitate thermal equilibration, and flame-sealed. Samples were kept frozen in liquid nitrogen for a few hours, until they were inserted into a precooled resonator. Continuous wave EPR spectra at 20 K were acquired at 9.3714 GHz on a Bruker E580 spectrometer with an SHQE resonator and equipped with a Bruker/ColdEdge Stinger cryogenic system. Spectra were acquired at 100 kHz, 2000 G scan width, a time constant of 82 ms, sweep time of 84 s with a 7 s delay to allow field settling at the end of each scan, and signal averaging of four scans. The microwave power was selected to be in a range where the signal increases linearly with square root of power. Simulations were performed using the Bruker BioSpin software Aniso-spin fit. The g values for two overlapping signals were adjusted manually using values reported for MftC as the starting points.[107]

Synthesis and Purification of Substrate TigB-3R

Fmoc-based solid phase syntheses of C-amidated peptide TvgA-4R and its variants were performed using CEM Liberty Blue Automated Microwave Peptide Synthesizer. All peptides were synthesized on a scale of 0.5 mmol with Rink Amide ProTide (LL) resin 100-200 mesh (0.18 mmol/g). A 2 M Standard Fmoc and tBu-protected amino acids were

prepared in N, N-Dimethylformamide (DMF). DMF was used as a wash buffer. The deprotection cocktail consisted of 10% piperazine (w/v) in the ratio of EtOH:N-Methyl-2-pyrrolidone (NMP) is 10:90. 0.5M N, N'-Diisopropylcarbodiimide (DIC) in DMF was utilized as an activator buffer. 0.5 M Oxyma in DMF was an activator base. Nitrogen (*gas*) was kept supplied during the synthesis. When the synthesis was completed, the resin was washed twice with 10 mL of methanol and once with 3 mL of chloroform. After drying under the vacuum, the resin was soaked in the 2 mL of cleavage cocktail which contains TFA:TIS:H_2O=95:2.5:2.5 for 35 min at 38 °C to cleave the peptide from the resin. The mixture was filtered into the cold 20 mL of diethyl ether and the peptides started precipitating at room temperature for 15 min centrifuging for 10 min at 4°C at 10000 rpm removes diethyl ether layer. The peptide pellet was resuspended in DMSO. Shimadzu UFLC was used to purify the crude peptide. The crude peptide was purified through a Semi-preparative 10×250 mm C4 15-20 μm reverse-phase column (Vydac 214TP152010) using 0.1% Formic acid and acetonitrile as mobile phase. The collection of different peaks was subjected to LC-MS. The aimed peptide collection was lyophilized overnight and kept in -20°C for further use.

Peptide Modification Reactions

TigB and TigE reactions were set up in an anaerobic chamber and all the reactants and reagents were prepared anaerobically. The synthesized and lyophilized TigB-3R was transferred and dissolved in DMSO. The concentrations of TigB-3R and TigE were determined by UV spectroscopy at 280 nm and 410 nm respectively (ε = 1.49 $mM^{-1}cm^{-1}$ and 45 $mM^{-1}cm^{-1}$). The reaction was set up with 10 mM DTT, 200 μM TigB-3R, 200 μM

TigE, 1mM NADPH, 10 μM Fld, 10 μM FldR, and 10 mM SAM, and in reaction buffer (50 mM HEPES, 300 mM NaCl, pH 8.0). An overnight reaction was carried out and quenched by 1% TFA. After centrifugation and filtration of the reaction mixture, the product was separated over HLPC by using a C_4 column (150 × 4.6 mm, 5 μm) (Phenomenex) with 0.1% formic acid (A) and acetonitrile (B) as mobile phases. The gradient program was as follows: 20–30% B (0-6 min), 30–50% B (6-11.5 min), 50–100% B (11.5-14 min), 100% B (14-15 min), and then 100%–20% B (15-17 min), 20% B (17-18min) at a flow rate of 1.0 mL/min and 35°C. The products were verified by LC-MS/MS. Wavelengths at 254 nm and 274 nm were monitored, and the chromatogram was reported at 274 nm.

HPLC Purifications

A UFLC (Shimadzu) equipped with pumps (LC-20AB), a column oven (CTO-20A), a control module (CBM-20A), and a detector (SPD-20A) was used to purify TigB-3R. Separation was carried out on a C_4 column (150 × 4.6 mm, 5 μm) (Phenomenex) The mobile phase consisted of 0.1% formic acid (A) and acetonitrile (B). The flow rate was 5.0 ml/min, and the elution was carried out with a gradient of 10–50% B (0-13 min), 50–100% B (13-16 min), 100–10% B (16-18 min) at 35°C.

LC-QToF-MS and MS/MS Analysis of Peptides

All mass spectrometry analyses were carried out on Shimadzu Prominence-i LC-2030 HPLC coupled to a Shimadzu LC-MS 9030 which is equipped with an ion accumulation (UFaccumulation), a grating (UFgrating), a funnel (Funnel MCP), a temperature-controlled

21

tube (UF-FlightTube), and a ToF (iRefTOF). An LC gradient described in the "Peptide modification reactions" section was used. The samples were verified by LC-QToF-MS with 4 kV ion spray voltage at 35 °C. Ionization was achieved using electrospray ionization (ESI) in positive mode. Tandem analysis was carried out on parent ions between 1625.15 amu to 1626.65 amu, using a collision energy of 80.8 keV, and a mass range of 200-2000 amu. Data was collected and processed by LabSolutions Insight and the UCSF Protein Prospector web server.

NMR Analyses of TigB-3R and Its Product.

The lyophilized starting material (TigB-3R) and product were prepared in 99.9% deuterated DMSO. NMR spectra were recorded on Bruker UltraShield 500/54 Plus spectrometer at the University of Denver. kHSQC data collection and residues assignment were processed using MestReNova v. 10.0.1 program (Mestrelab Research).

CHAPTER THREE: RESULTS

A family of CP Synthases

We expanded our bioinformatic analysis of TvgB homologues and found at least six subfamilies of related BGCs. To find TvgB homologues, we used the radical-SAM.org webtool and ran a BLAST search of TvgB homologue (Uniprot: S2KMD3).[108] From this, we identified a sequence similarity network (SSN) cluster (1-1-201:AS65) that defined TvgB as well as 49 other Uniprot IDs. Using the Genome Neighborhood Diagram tool,[109] all available precursor peptides in the intergenic regions were identified and the conserved repeating regions of the peptide sequences were mapped to each TvgB homologue. The SSN was then reorganized by peptide sequence to yield the network shown in Figure 5A. From this analysis at least six conserved sequence motifs within the TvgB family of RiPP BGCs were identified. Interestingly, in each case a Val or Ile is conserved, suggesting that rSAM enzymes represented in this network could be a family of cyclopropyl (CP) synthases.
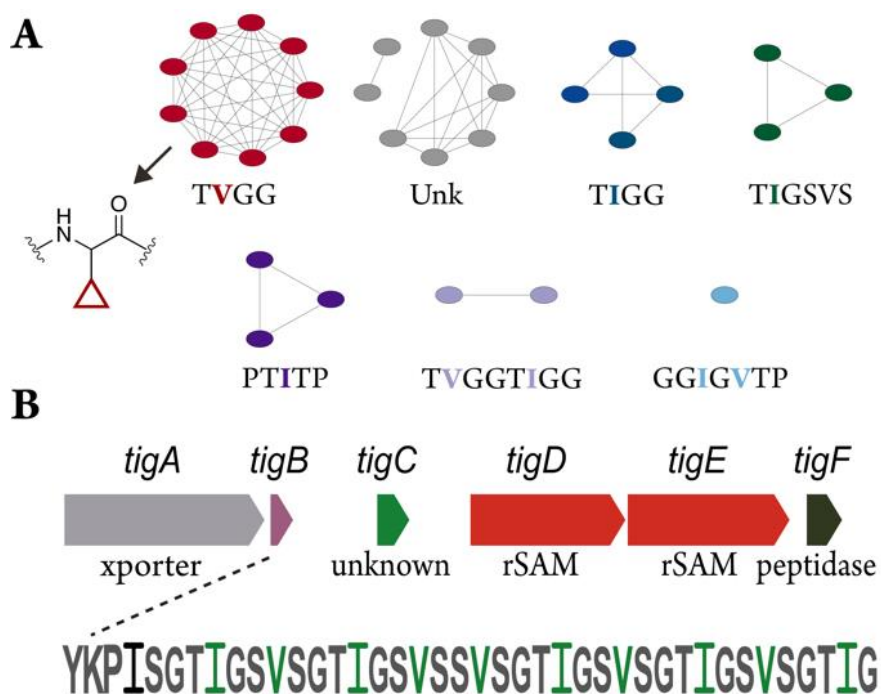
Figure 5. Bioinformatic analysis of the family of cyclopropyl synthases. A) The SSN of cluster 1-1-201:AS65 from radical-SAM.org was sorted by the associated RiPP pathway precursor peptide repeating sequence. From this, at least six distinct RiPP families that require putative cyclopropyl synthases were discovered. B) The TIG biosynthetic pathway with TigB that contains a TIGSVS repeating sequence.

The TIGSVS Subfamily

To provide evidence that the SSN network does represent a family of CP synthases, we characterized a rSAM enzyme from the TIGSVS biosynthetic gene cluster (BGC). We chose the TIGSVS BGC because it had unique features. First it encoded a distinct transporter, two rSAM enzymes (*tigD* and *tigE*) and a peptidase. The gene, *TigC*, appears to be an orphan and does not have any homologues. Second, the 60-amino acid precursor peptide, TigB, consists of a TIGSVS motif that is repeated up to five times, suggesting that five identical products were formed from the peptide (Figure 5B). We expected that either

TigD and/or TigE would catalyze the formation of a cyclopropane on the conserved Ile and/or Val residues, similar to what we showed for TVG biosynthesis.

Characterization of TigE and the TigE Reaction

To determine if our hypothesis was correct, we reconstituted enzymatic activity in the pathway rSAM enzyme, TigE. The His-tagged protein was recombinantly expressed in *E. coli*, purified anaerobically using immobilized metal affinity chromatography, and reconstituted with iron and sulfide (Figure 6A). The UV-Vis spectrum of the reconstituted protein showed a peak absorbance at 410 nm (Figure 6B), consistent with the incorporation of [4Fe-4S] clusters. Further characterization of the iron-sulfur clusters by EPR spectroscopy show that that reduced form of TigE contains two iron-sulfur cluster species each with distinct g values and linewidths (Figure 6C). This suggests that at least one [4Fe-4S] cluster has a significantly different environment compared to the remaining cluster(s). A potential explanation for this feature will be discussed later.
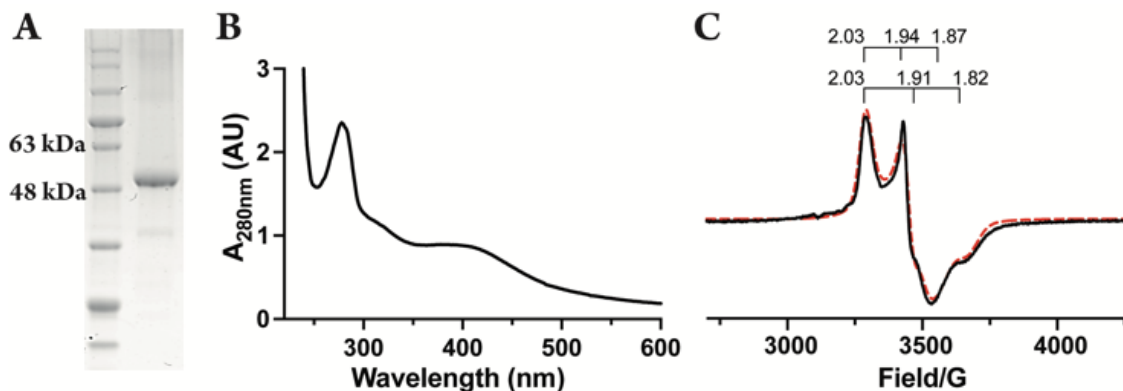
Figure 6. Characterization of TigE protein. A) An SDS-PAGE gel showing that purified TigE is nearly homogenous. B) The appearance of a 410 nm shoulder in the absorbance spectra of reconstituted TigE suggests that [4Fe-4S] clusters are present. C) The X-band (9.3715 GHz) CW spectrum (black) of reduced TigE at 20 K. The simulation of the data (red dashes)

Next, we set up reactions with TigE. We used microwave assisted solid phase peptide synthesis to attain a truncated TigB peptide with three repeating TIGSVS motifs and an N-terminal Trp to increase absorbance (herein referred to as TigB-3R). The C-terminally amidated peptide was purified by HPLC and the mass of TigB-3R was validated by LCMS (observed $[M+2H]^{2+}$ m/z: 1627.8739, Δppm 13.0). To evaluate enzymatic activity, reactions were set up containing TigE, TigB-3R, SAM, dithiothreitol (DTT), and dithionite (DTH). Unexpectedly, a change in the retention time and mass of TigB-3R were not observed by HPLC or LC-MS, respectively. It is known that some rSAM enzymes are only active in vitro with the flavodoxin (FldA)/flavodoxin reductase (Fpr) system.[110] Accordingly, the *E. coli* FldA and Fpr proteins were recombinantly expressed in and purified from *E. coli.* New overnight reactions with TigE were set up substituting DTH with FldA, Fpr, and NADPH. The reactions were then quenched and evaluated by HPLC and LCMS. This time, changes in the retention time of the peptide were observed in HPLC chromatograms, with three new peaks resolving at 8.25 min, 8.0 min, and 7.5 min (Figure 7A). Further analysis of the reactions by LCMS showed the appearance of three mass new species corresponding to the loss of -2H (observed $[M+2H]^{2+}$ m/z: 1626.8674, Δppm 13.9), -4H (observed $[M+2H]^{2}$ m/z: 1625.8597, Δppm 14.0), and -6H (observed $[M+2H]^{2}$ m/z: 1624.8515, Δppm 13.7). These masses are consistent with the formation of one, two, and three intramolecular bonds (Figure 7B).
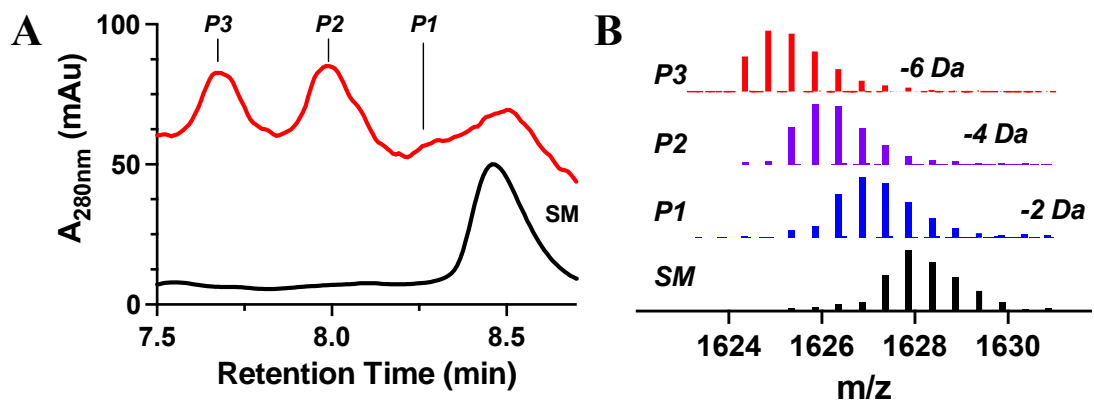
Figure 7. LC-MS analysis of overnight TigE reaction with TigB-3R. A) Stacked LC chromatogram of unmodified (black) and modified (red) peptide TigB-3R. SM, starting material. P, product. B) HR-MS spectra of [M+2H]2+ ions of substrate TigB-3R and three formed products. From the bottom to the top: TigB-3R (black), one modification product (blue), two modifications product (purple), and three modifications product (red).

To determine the site of TigE modification, an LC-MS/MS analysis was performed on the $[M+2H]^{2+}$ ion of unmodified and modified TigB-3R with the loss of 6H. To do so, the purified product of overnight reaction was applied to LC-MS/MS. The MS/MS data yielded both *b-* and *y-*fragments with the amino acid coverage of the peptide. The N-terminal *b-*fragments of all three products were unchanged. This indicates the modification occurred on the repetitive TIGSVS sequence. The *y-*fragment data showed that the last Ile residue was modified by 2 Da lost. By analyzing the 4 Da and 6 Da lost products, we found that TigE modified the Ile residue of TigB-3R in a non-processive order (Figure 8, Table 3-7). To confirm that Ile is the modified residue, we mutated all the Ile to Ala, (I to A)4 TigB-3R (Table 8) and reacted with TigE. As expected, we saw no mass change on the peptide.
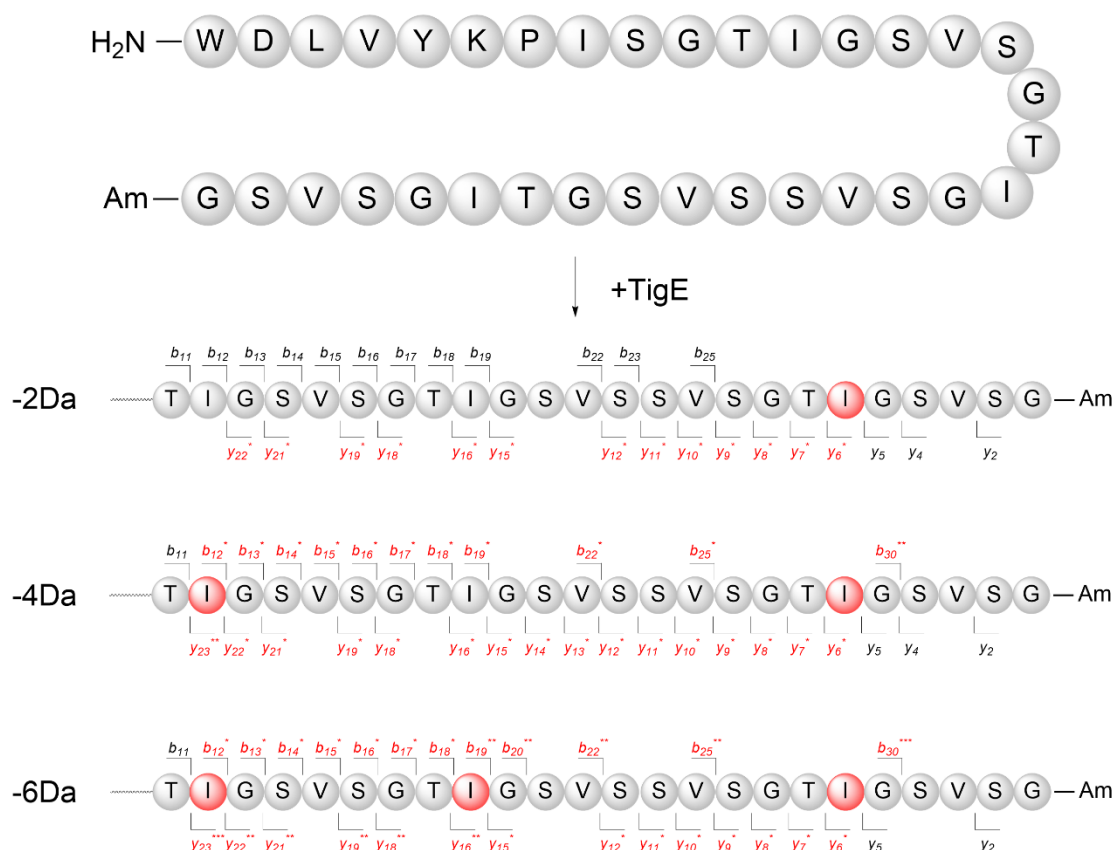
Figure 8. HR-LC-MS/MS fragmentation pattern of substrate TigB-3R and TigE products with one, two, and three modifications. Fragments with one, two, and three asterisks are indicative of the loss of 2 Da, 4 Da, and 6 Da respectively.

Determining the Structure of the TigE Product

After determining the location of the modification on the TigB-3R peptide, we next sought to determine the structure of the modification. We expected that TigE belongs to a family of CP synthases and it is forming a methyl-CPG moiety from Ile. To test this hypothesis, we carried out the TigE reactions on a large scale, purified the reaction product, and collected ^{1}H NMR spectra on the reaction product. Assessment of the unmodified and modified TigB-3R by ^{1}H NMR revealed new features in the lower frequency range (~3.65 ppm δH and <1 ppm δH, Fig 9A and 9B). The chemical shifts at δH ~0.58 and 0.15 ppm

are consistent with those found for Val C_γ's that contribute to the cyclopropane ring in the TVG biosynthetic pathway.[92] Therefore, we expect that the pair of low frequency chemical shifts correspond to the Ile C_γ's belonging to a cyclopropane ring. In addition, a new doublet species at δH 0.9 ppm was observed. We expect that the double belonged to C_δ of Ile. Lastly, we observed a new species at δH 3.65 ppm which we expect belongs to Ile C_δ, which is also consistent with our previous findings.[92]

To provide more concrete evidence that TigE could catalyze the formation of a methyl-CPG from Ile, we carried out ^{13}C HSQC experiments using the isotopically labeled peptide ($^{13}C_6$, ^{15}N-Ile)$_3$-TigB-3R, referred to as ^{13}C-TigB-3R herein. Differences in the ^{13}C HSQC spectra of the starting material and the TigE product (Figure 9C and D) were most prominent in the upfield region. We observed a new coupled feature at (δH 3.75 ppm; δC 55.79 ppm) in the ^{13}C HSQC spectra which is consistent with the C_α of methyl-CPG. We also observed new coupled features in the ^{13}C HSQC spectra of the product at (δH 0.19 ppm; δC 10.54 ppm) and (δH 0.61 ppm; δC 10.54 ppm). These features are consistent with the C_γ's of methyl-CPG. Lastly, from the ^{13}C HSQC spectra of the product, we assigned the feature at (δH 0.97 ppm; δC 17.91 ppm) as the C_δ and the feature at (δH 0.65 ppm; δC 21.23) as C_β.
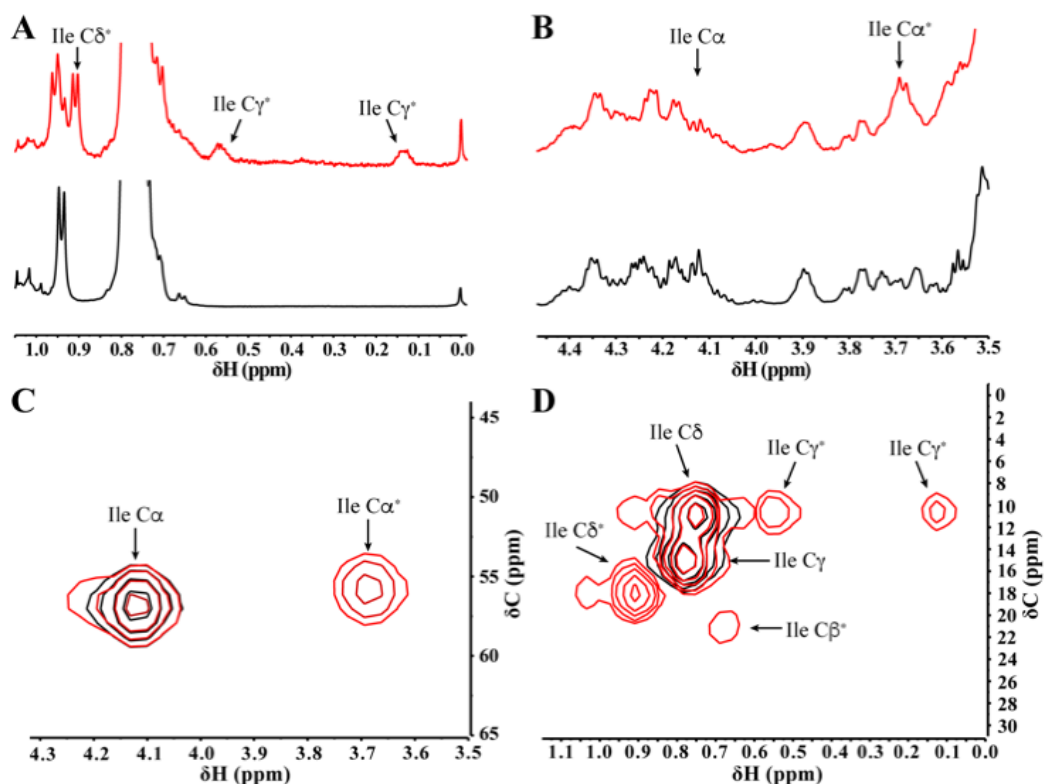
Figure 9. Structural elucidation of the modified TigB-3R. A, B) Stack of 1H NMR spectra for the peptide variant (13C6, 15N-Ile)3-TigB-3R (black) and TigE product (red). C, D) 13C HSQC strips of overlaid spectra of peptide (black) and product (red) for the peptide variant (13C6, 15N-Ile)3-TigB-3R (black) and TigE product (red).

Taken together, the MS analysis showing the incremental loss of 2, 4, and 6 Da, the localization of the modifications to Ile by MS/MS, and the 1D and 2D NMR experiments indicate that TigE installs a carbon-carbon bond between the Ile C_γ's on the precursor peptide TigB, yielding methyl-CPG (Figure 13-16).
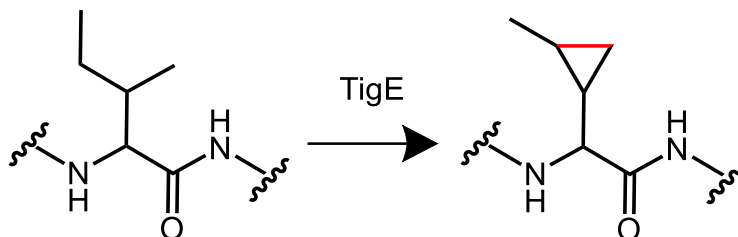
Figure 10. A schematic representation of modification catalyzed by TigE.

Structural Characterization of TigE

Working with Prof. Tyler Grove, we have a structure of TigE (Figure 11). The N-terminus of TigE is a parallel β/α partial triose phosphate isomerase (TIM) barrel. Although the structure of the TigE rSAM domain is partially solved, we found a potential active [4Fe-4S] cluster binding site. In the sequence alignment of TigE and the anSME, there is a conserved radical sequence motif, a $CX_3CX\Phi C$ motif, in which Φ is an aromatic residue and X is a random amino acid. In anSME, C15, C19, and C22 each ligates an iron atom in one of the [4Fe-4S] clusters which are conserved in TigE as C120, C124 and C127.[111] Downstream of the RS domain is the SPASM domain. Within the SPASM domain, residues C360, C377, C427, and Y339 appear to coordinate the Aux I cluster. Each residue resides within a distance of 3.316 Å, 2.318 Å, 2.46 Å, and 2.194 Å respectively (Figure 12A). Of note, this is the first reported instance of a tyrosine conjugate a Fe-S cluster in rSAM-SPASM domain.

Within the C-terminus of SPASM domain, C414, C417, C423, and C446 cooperate with Aux II cluster. Each residue locates within a distance of 2.197 Å, 2.298 Å, 2.275 Å, and 2.356 Å respectively (Figure 12B). Both Aux I and Aux II share a highly conserved $CX_2CX_5CX_3C$ motif (C414-C427). Within this motif, one cysteine ligates to Aux I and three cysteines interact with Aux II. The first three cysteines (C414, C417, and C423) of the motif provide three ligands to the second auxiliary cluster, Aux II. This phenomenon was also observed in anSME.[111]
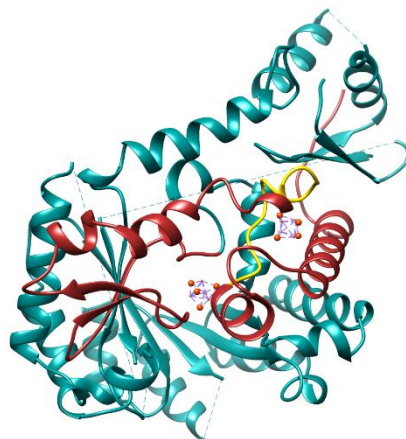
Figure 11. A cartoon of our initial TigE structure solved at 1.74 Å. The structure shows RS domain (dark cyan) that contains the β/α TIM barrel and a SPASM domain (brown) comprises the CX2CX5CX3C motif (gold) that couples two auxiliary clusters (orange).

A   **B**
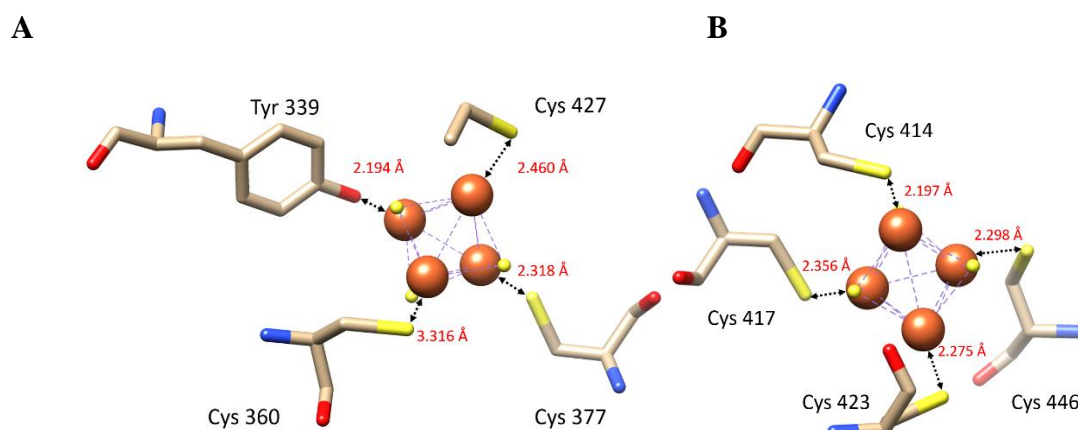
Figure 12. Auxiliary clusters binding site in SPASM domain. A) AxuI interacts with Cys360, Cys377, Cys427 and Tyr339. B) AuxII interacts with Cys414, Cys417, Cys423 and Cys446. The auxiliary clusters are shown as a ball and stick representation with iron atoms colored orange and sulfur atoms colored yellow.

CHAPTER FOUR: DISCUSSION AND SUMMARY

Currently, most rSAM-dependent RiPPs that have been characterized are derived from Haft and Basu's initial bioinformatic study.[63] While still lots of RiPPs biosynthetic pathway remain uncharacterized. Since 2011, many online RiPPs mining tools are designed to expand the understanding of different rSAM-dependent RiPPs. In this study, EFI-EST and EFI-GNT, and the recently launched radicalSAM.org were applied in the sereaching of new rSAM-dependent RiPPs.[112] With these advanced mining tools, we have published a CP synthase, TvgB, in TVG biosynthetic pathway in the BGC associated with Cluster 40.[92] We targeted an other pathway in Cluster 40 a peptide with a highly conserved TIGSVS repeating motif. We found this motif to be peculiar because of its repeating nature and 2 rSAM enzymes. Therefore, we cloned, expressed, and purified the rSAM associated with the TIG biosynthetic cluster. We reconstituted TigE enzymatic activity with a truncated TigB peptide and solved the structure of the modified peptide. By doing so, we discovered a new RiPP topology that is based on the formation of methyl-CPG. Interestingly, the installation of methyl-CPG by TigE is repeated multiple times in the precursor peptide. Considering the composition of the biosynthetic cluster, it is likely that the TigB encodes for multiple small molecule products based on the TIGSVS motif. We expect that TigF could hydrolyze the maturing product and export it to the extracellular matrix. What we described here is, so far, TigE, the rSAM enzyme in TIG biosynthetic pathway, is a CP synthase that installs the methyl-CPG from Ile.

To determine the structural elements that define a CP synthase, we have carried out a structure-function analysis of TigE. This is conceptually innovative because it will establish the paradigm for defining a CP synthase. We found that the phenol of Tyr339 coordinates an auxiliary Fe-S cluster proximal to the active site, the first of its kind in rSAM enzymes. We expect that Tyr339 could be a bioinformatic marker for discovering new CP synthase dependent RiPPs since Tyr339 is conserved in TvgB (35% sequence identity). Tyr339 could serve as the H• donor for the redox neutral reaction. If this is the case, the reaction would likely pass through a tyrosyl radical.

In summary, we reported on an updated bioinformatics characterization of the rSAM subfamily IPR023867. We describe multiple rSAM-dependent RiPP biosynthetic pathways that, despite being based on known chemical linkages, are expected to result in unprecedented RiPP topologies. Moreover, we made available the resources (e.g. SSN file, GNT files, tables) to broaden the focus of rSAM-dependent RiPP discovery. Lastly, we utilized our SSN results to discover the first poly-methyl-CPG containing RiPP product installed by the rSAM enzyme, TigE. Future work will entail solving the mechanism of TigE and the product of the pathway.

REFERENCES

(1)   Montalbán-López, M.; A. Scott, T.; Ramesh, S.; R. Rahman, I.; Heel, A. J.van; H. Viel, J.; Bandarian, V.; Dittmann, E.; Genilloud, O.; Goto, Y.; Burgos, M. J. G.; Hill, C.; Kim, S.; Koehnke, J.; A. Latham, J.; James Link, A.; Martínez, B.; K. Nair, S.; Nicolet, Y.; Rebuffat, S.; Sahl, H.-G.; Sareen, D.; W. Schmidt, E.; Schmitt, L.; Severinov, K.; D. Süssmuth, R.; W. Truman, A.; Wang, H.; Weng, J.-K.; Wezel, G. P.van; Zhang, Q.; Zhong, J.; Piel, J.; A. Mitchell, D.; P. Kuipers, O.; Donk, W. A.van der.New Developments in RiPP Discovery, Enzymology and Engineering. *Nat. Prod. Rep.* **2020**. https://doi.org/10.1039/D0NP00027B.

(2)   B, F.; C, G.; A, G.; J, V.; P, N.; C, B.; L, F.; P, H.; N, L.-B.; V, M.; R, G.Rgg Proteins Associated with Internalized Small Hydrophobic Peptides: A New Quorum-Sensing Mechanism in Streptococci. *Mol. Microbiol.* **2011**, *80* (4), 1102–1119. https://doi.org/10.1111/J.1365-2958.2011.07633.X.

(3)   Haft, D. H.Bioinformatic Evidence for a Widely Distributed, Ribosomally Produced Electron Carrier Precursor, Its Maturation Proteins, and Its Nicotinoprotein Redox Partners. *BMC Genomics* **2011**, *12* (1), 21. https://doi.org/10.1186/1471-2164-12-21.

(4)   Anthony, C.Pyrroloquinoline Quinone (PQQ) and Quinoprotein Enzymes. *https://home.liebertpub.com/ars* **2004**, *3* (5), 757–774. https://doi.org/10.1089/15230860152664966.

(5)   Fleuchot, B.; Gitton, C.; Guillot, A.; Vidic, J.; Nicolas, P.; Besset, C.; Fontaine, L.; Hols, P.; Leblond-Bourget, N.; Monnet, V.; Gardan, R.Rgg Proteins Associated with Internalized Small Hydrophobic Peptides: A New Quorum-Sensing Mechanism in Streptococci. *Mol. Microbiol.* **2011**, *80* (4), 1102–1119. https://doi.org/10.1111/j.1365-2958.2011.07633.x.

(6)   Bushin, L. B.; Clark, K. A.; Pelczer, I.; Seyedsayamdost, M. R.Charting an Unexplored Streptococcal Biosynthetic Landscape Reveals a Unique Peptide Cyclization Motif. *J. Am. Chem. Soc.* **2018**, *140* (50), 17674–17684. https://doi.org/10.1021/jacs.8b10266.

(7)   Schramma, K. R.; Bushin, L. B.; Seyedsayamdost, M. R.Structure and Biosynthesis of a Macrocyclic Peptide Containing an Unprecedented Lysine-to-Tryptophan Crosslink. *Nat. Chem.* **2015**, *7* (5), 431–437. https://doi.org/10.1038/nchem.2237.

(8)   Hudson, G. A.; Mitchell, D. A.RiPP Antibiotics: Biosynthesis and Engineering Potential. *Curr. Opin. Microbiol.* **2018**, *45*, 61. https://doi.org/10.1016/j.mib.2018.02.010.

(9)   Ayikpoe, R.; Latham, J. A.MftD Catalyzes the Formation of a Biologically Active Redox Center in the Biosynthesis of the Ribosomally Synthesized and Post-Translationally Modified Redox Cofactor, Mycofactocin. *J. Am. Chem. Soc.* **2019**, *141*, 13582–13591.

(10)   Zhu, W.; Klinman, J. P.Biogenesis of the Peptide-Derived Redox Cofactor Pyrroloquinoline Quinone. *Curr. Opin. Chem. Biol.* **2020**, *59*, 93–103. https://doi.org/10.1016/j.cbpa.2020.05.001.

(11)   Takase, S.; Kurokawa, R.; Kondoh, Y.; Honda, K.; Suzuki, T.; Kawahara, T.; Ikeda, H.; Dohmae, N.; Osada, H.; Shin-Ya, K.; Kushiro, T.; Yoshida, M.; Matsumoto, K.Mechanism of Action of Prethioviridamide, an Anticancer Ribosomally Synthesized and Post-Translationally Modified Peptide with a Polythioamide Structure. *ACS Chem. Biol.* **2019**, *14* (8), 1819–1828. https://doi.org/10.1021/ACSCHEMBIO.9B00410/ASSET/IMAGES/LARGE/CB-2019-00410Z_0006.JPEG.

(12)   Graham A., H.; Douglas A., M.RiPP Antibiotics: Biosynthesis and Engineering Potential. *Curr. Opin. Microbiol. 45*, 61. https://doi.org/10.1016/j.mib.2018.02.010.

(13)   Latham, J. A.; Iavarone, A. T.; Barr, I.; Juthani, P.V.; Klinman, J. P.PqqD Is a Novel Peptide Chaperone That Forms a Ternary Complex with the Radical S-Adenosylmethionine Protein PqqE in the Pyrroloquinoline Quinone Biosynthetic Pathway. *J. Biol. Chem.* **2015**, *290* (20), 12908–12918. https://doi.org/10.1074/jbc.M115.646521.

(14)   Manuel, M.-L.; Thomas, A. S.; Sangeetha, R.; Imran, R. R.; Auke J. van, H.; Jakob, H. V.; Vahe, B.; Elke, D.; Olga, G.; Yuki, G.; María José Grande, B.; Colin, H.; Seokhee, K.; Jesko, K.; John, A. L.; A., J. L.; Beatriz, M.; Satish, K. N.; Yvain, N.; Sylvie, R.; Hans-Georg, S.; Dipti, S.; Eric, W. S.; Lutz, S.; Konstantin, S.; Roderich, D. S.; Andrew, W. T.; Huan, W.; Jing-Ke, W.; Gilles P. van, W.; Qi, Z.; Jin, Z.; Jörn, P.; Douglas, A. M.; Oscar, P. K.; Wilfred A. van der, D.New Developments in RiPP Discovery, Enzymology and Engineering. *Nat. Prod. Rep.* https://doi.org/10.1039/D0NP00027B.

(15)   Rowe, S. M.; Spring, D. R.The Role of Chemical Synthesis in Developing RiPP Antibiotics. *Chem. Soc. Rev.* **2021**, *50* (7), 4245–4258. https://doi.org/10.1039/D0CS01386B.

(16)   McAuliffe, O.; Ross, R. P.; Hill, C.Lantibiotics: Structure, Biosynthesis and Mode of Action. *FEMS Microbiol. Rev.* **2001**, *25* (3), 285–308. https://doi.org/10.1111/J.1574-6976.2001.TB00579.X.

(17)   Salomon, R. A.; Farias, R. N.Microcin 25, a Novel Antimicrobial Peptide Produced by Escherichia Coli. *J. Bacteriol.* **1992**, *174* (22), 7428–7435. https://doi.org/10.1128/JB.174.22.7428-7435.1992.

(18)   Cheng, C.; Hua, Z. C.Lasso Peptides: Heterologous Production and Potential Medical Application. *Front. Bioeng. Biotechnol.* **2020**, *8*, 1131. https://doi.org/10.3389/FBIOE.2020.571165/BIBTEX.

(19)   Li, Y.; Ducasse, R.; Zirah, S.; Blond, A.; Goulard, C.; Lescop, E.; Giraud, C.; Hartke, A.; Guittet, E.; Pernodet, J. L.; Rebuffat, S.Characterization of Sviceucin from Streptomyces Provides Insight into Enzyme Exchangeability and Disulfide Bond Formation in Lasso Peptides. *ACS Chem. Biol.* **2015**, *10* (11), 2641–2649. https://doi.org/10.1021/ACSCHEMBIO.5B00584.

(20)   Svangård, E.; Burman, R.; Gunasekera, S.; Lövborg, H.; Gullbo, J.; Göransson, U.Mechanism of Action of Cytotoxic Cyclotides: Cycloviolacin O2 Disrupts Lipid Membranes. *J. Nat. Prod.* **2007**, *70* (4), 643–647. https://doi.org/10.1021/NP070007V.

(21)   Williams, A. B.; Jacobs, R. S.A Marine Natural Product, Patellamide D, Reverses Multidrug Resistance in a Human Leukemic Cell Line. *Cancer Lett.* **1993**, *71* (1–3), 97–102. https://doi.org/10.1016/0304-3835(93)90103-G.

(22)   Fu, X.; Do, T.; Schmitz, F. J.; Andrusevich, V.; Engel, M. H.New Cyclic Peptides from the Ascidian Lissoclinum Patella. *J. Nat. Prod.* **1998**, *61* (12), 1547–1551. https://doi.org/10.1021/NP9802872.

(23)   Hetrick, K. J.; van derDonk, W. A.Ribosomally Synthesized and Post-Translationally Modified Peptide Natural Product Discovery in the Genomic Era. *Curr. Opin. Chem. Biol.* **2017**, *38*, 36–44. https://doi.org/10.1016/j.cbpa.2017.02.005.

(24)   Ortega, M. A.; van derDonk, W. A.New Insights into the Biosynthetic Logic of Ribosomally Synthesized and Post-Translationally Modified Peptide Natural Products. *Cell Chem. Biol.* **2016**, *23* (1), 31–44. https://doi.org/10.1016/j.chembiol.2015.11.012.

(25)   Yang, X.; Van DerDonk, W. a.Ribosomally Synthesized and Post-Translationally Modified Peptide Natural Products: New Insights into the Role of Leader and Core Peptides during Biosynthesis. *Chem. - A Eur. J.* **2013**, *19*, 7662–7677. https://doi.org/10.1002/chem.201300401.

(26)   Arnison, P. G.; Bibb, M. J.; Bierbaum, G.; Bowers, A. A.; Bugni, T. S.; Bulaj, G.; Camarero, J. A.; Campopiano, D. J.; Challis, G. L.; Clardy, J.; Cotter, P. D.; Craik, D. J.; Dawson, M.; Dittmann, E.; Donadio, S.; Dorrestein, P. C.; Entian, K.-D.; Fischbach, M. A.; Garavelli, J. S.; Göransson, U.; Gruber, C. W.; Haft, D. H.; Hemscheidt, T. K.; Hertweck, C.; Hill, C.; Horswill, A. R.; Jaspars, M.; Kelly, W. L.; Klinman, J. P.; Kuipers, O. P.; Link, A. J.; Liu, W.; Marahiel, M. A.; Mitchell, D. A.; Moll, G. N.; Moore, B. S.; Müller, R.; Nair, S. K.; Nes, I. F.; Norris, G. E.; Olivera, B. M.; Onaka, H.; Patchett, M. L.; Piel, J.; Reaney, M. J. T.; Rebuffat, S.; Ross, R. P.; Sahl, H.-G.; Schmidt, E. W.; Selsted,

M. E.; Severinov, K.; Shen, B.; Sivonen, K.; Smith, L.; Stein, T.; Süssmuth, R. D.; Tagg, J. R.; Tang, G.-L.; Truman, A. W.; Vederas, J. C.; Walsh, C. T.; Walton, J. D.; Wenzel, S. C.; Willey, J. M.; van derDonk, W. A.Ribosomally Synthesized and Post-Translationally Modified Peptide Natural Products: Overview and Recommendations for a Universal Nomenclature. *Nat. Prod. Rep.* **2013**, *30* (1), 108–160. https://doi.org/10.1039/C2NP20085F.

(27)   Patton, G. C.; Paul, M.; Cooper, L. E.; Chatterjee, C.; Van DerDonk, W. A.The Importance of the Leader Sequence for Directing Lanthionine Formation in Lacticin 481. *Biochemistry* **2008**, *47* (28), 7342–7351. https://doi.org/10.1021/BI800277D.

(28)   Yang, X. P.; Zhong, G. F.; Lin, J. P.; Mao, D.Bin; Wei, D. Z.Pyrroloquinoline Quinone Biosynthesis in Escherichia Coli through Expression of the Gluconobacter Oxydans PqqABCDE Gene Cluster. *J. Ind. Microbiol. Biotechnol.* **2010**, *37* (6), 575–580. https://doi.org/10.1007/S10295-010-0703-Z.

(29)   Latham, J. A.; Iavarone, A. T.; Barr, I.; Juthani, P.V.; Klinman, J. P.PqqD Is a Novel Peptide Chaperone That Forms a Ternary Complex with the Radical S-Adenosylmethionine Protein PqqE in the Pyrroloquinoline Quinone Biosynthetic Pathway. *J. Biol. Chem.* **2015**, *290* (20), 12908–12918. https://doi.org/10.1074/JBC.M115.646521.

(30)   Altschul, S. F.; Madden, T. L.; Schäffer, A. A.; Zhang, J.; Zhang, Z.; Miller, W.; Lipman, D. J.Gapped BLAST and PSI-BLAST: A New Generation of Protein Database Search Programs. *Nucleic Acids Res.* **1997**, *25* (17), 3389–3402. https://doi.org/10.1093/NAR/25.17.3389.

(31)   Sudek, S.; Haygood, M. G.; Youssef, D. T. A.; Schmidt, E. W.Structure of Trichamide, a Cyclic Peptide from the Bloom-Forming Cyanobacterium Tnchodesmium Erythraeum, Predicted from the Genome Sequence. *Appl. Environ. Microbiol.* **2006**, *72* (6), 4382–4387.   https://doi.org/10.1128/AEM.00380-06/SUPPL_FILE/SUPPORTING_MATERIALREVISED.ZIP.

(32)   Begley, M.; Cotter, P. D.; Hill, C.; Ross, R. P.Identification of a Novel Two-Peptide Lantibiotic, Lichenicidin, Following Rational Genome Mining for LanM Proteins. *Appl. Environ. Microbiol.* **2009**, *75* (17), 5451–5460. https://doi.org/10.1128/AEM.00730-09/ASSET/339067F5-7DF3-4D26-98A4-12555B578B16/ASSETS/GRAPHIC/ZAM0170902170003.JPEG.

(33)   deJong, A.; vanHijum, S. A. F. T.; Bijlsma, J. J. E.; Kok, J.; Kuipers, O. P.BAGEL: A Web-Based Bacteriocin Genome Mining Tool. *Nucleic Acids Res.* **2006**, *34* (Web Server issue), W273. https://doi.org/10.1093/NAR/GKL237.

(34)   vanHeel, A. J.; deJong, A.; Song, C.; Viel, J. H.; Kok, J.; Kuipers, O. P.BAGEL4: A User-Friendly Web Server to Thoroughly Mine RiPPs and Bacteriocins. *Nucleic Acids Res.* **2018**, *46* (W1), W278–W281. https://doi.org/10.1093/nar/gky383.

(35)   Zhong, Z.; He, B.; Li, J.; Li, Y. X.Challenges and Advances in Genome Mining of Ribosomally Synthesized and Post-Translationally Modified Peptides (RiPPs). *Synth. Syst. Biotechnol.* **2020**, *5* (3), 155–172. https://doi.org/10.1016/J.SYNBIO.2020.06.002.

(36)   Tietz, J. I.; Schwalen, C. J.; Patel, P. S.; Maxson, T.; Blair, P. M.; Tai, H.-C.; Zakai, U. I.; Mitchell, D. A.A New Genome-Mining Tool Redefines the Lasso Peptide Biosynthetic Landscape. *Nat. Chem. Biol.* **2017**, *13* (5), 470–478. https://doi.org/10.1038/nchembio.2319.

(37)   Graham A., H.; Brandon J., B.; Adam J., D.; Christopher J., S.; Bryce, K.; Taras V., P.; Douglas A., M.Bioinformatic Mapping of Radical *S* -Adenosylmethionine-Dependent Ribosomally Synthesized and Post-Translationally Modified Peptides Identifies New Cα, Cβ, and Cγ-Linked Thioether-Containing Peptides. *J. Am. Chem. Soc.* **2019**, jacs.9b01519. https://doi.org/10.1021/jacs.9b01519.

(38)   vanHeel, A. J.; deJong, A.; Montalbán-López, M.; Kok, J.; Kuipers, O. P.BAGEL3: Automated Identification of Genes Encoding Bacteriocins and (Non-)Bactericidal Posttranslationally Modified Peptides. *Nucleic Acids Res.* **2013**, *41* (Web Server issue), W448. https://doi.org/10.1093/NAR/GKT391.

(39)   RODEO : Rapid ORF Description & Evaluation Online http://www.ripp.rodeo/manual.html (accessed May 18, 2022).

(40)   Gerlt, J. A.; Bouvier, J. T.; Davidson, D. B.; Imker, H. J.; Sadkhin, B.; Slater, D. R.; Whalen, K. L.Enzyme Function Initiative-Enzyme Similarity Tool (EFI-EST): A Web Tool for Generating Protein Sequence Similarity Networks. *Biochim. Biophys. Acta - Proteins Proteomics* **2015**, *1854* (8), 1019–1037. https://doi.org/10.1016/j.bbapap.2015.04.015.

(41)   Navarro-Muñoz, J. C.; Selem-Mojica, N.; Mullowney, M. W.; Kautsar, S. A.; Tryon, J. H.; Parkinson, E. I.; DeLos Santos, E. L. C.; Yeong, M.; Cruz-Morales, P.; Abubucker, S.; Roeters, A.; Lokhorst, W.; Fernandez-Guerra, A.; Cappelini, L. T. D.; Goering, A. W.; Thomson, R. J.; Metcalf, W. W.; Kelleher, N. L.; Barona-Gomez, F.; Medema, M. H.A Computational Framework to Explore Large-Scale Biosynthetic Diversity. *Nat. Chem. Biol.* **2020**, *16* (1), 60–68. https://doi.org/10.1038/S41589-019-0400-9.

(42)   Blin, K.; Medema, M. H.; Kazempour, D.; Fischbach, M. A.; Breitling, R.; Takano, E.; Weber, T.AntiSMASH 2.0—a Versatile Platform for Genome Mining of

Secondary Metabolite Producers. *Nucleic Acids Res.* **2013**, *41* (W1), W204–W212. https://doi.org/10.1093/nar/gkt449.

(43)   Skinnider, M. A.; Merwin, N. J.; Johnston, C. W.; Magarvey, N. A.PRISM 3: Expanded Prediction of Natural Product Chemical Structures from Microbial Genomes. *Nucleic Acids Res.* **2017**, *45* (W1), W49–W54. https://doi.org/10.1093/NAR/GKX320.

(44)   Skinnider, M. A.; Johnston, C. W.; Edgar, R. E.; Dejong, C. A.; Merwin, N. J.; Rees, P. N.; Magarvey, N. A.Genomic Charting of Ribosomally Synthesized Natural Product Chemical Space Facilitates Targeted Mining. *Proc. Natl. Acad. Sci. U. S. A.* **2016**, *113* (42), E6343–E6351. https://doi.org/10.1073/PNAS.1609014113.

(45)   Blin, K.; Wolf, T.; Chevrette, M. G.; Lu, X.; Schwalen, C. J.; Kautsar, S. A.; Suarez Duran, H. G.; DeLos Santos, E. L. C.; Kim, H. U.; Nave, M.; Dickschat, J. S.; Mitchell, D. A.; Shelest, E.; Breitling, R.; Takano, E.; Lee, S. Y.; Weber, T.; Medema, M. H.AntiSMASH 4.0-Improvements in Chemistry Prediction and Gene Cluster Boundary Identification.   *Nucleic   Acids   Res.*   **2017**,   *45*   (W1),   W36–W41. https://doi.org/10.1093/NAR/GKX319.

(46)   Blin, K.; Shaw, S.; Steinke, K.; Villebro, R.; Ziemert, N.; Lee, S. Y.; Medema, M. H.; Weber, T.AntiSMASH 5.0: Updates to the Secondary Metabolite Genome Mining Pipeline.   *Nucleic   Acids   Res.*   **2019**,   *47*   (W1),   W81–W87. https://doi.org/10.1093/NAR/GKZ310.

(47)   Agrawal, P.; Khater, S.; Gupta, M.; Sain, N.; Mohanty, D.RiPPMiner: A Bioinformatics Resource for Deciphering Chemical Structures of RiPPs Based on Prediction of Cleavage and Cross-Links. *Nucleic Acids Res.* **2017**, *45* (W1), W80–W88. https://doi.org/10.1093/NAR/GKX408.

(48)   Merwin, N. J.; Mousa, W. K.; Dejong, C. A.; Skinnider, M. A.; Cannon, M. J.; Li, H.; Dial, K.; Gunabalasingam, M.; Johnston, C.; Magarvey, N. A.DeepRiPP Integrates Multiomics Data to Automate Discovery of Novel Ribosomally Synthesized Natural Products.   *Proc.   Natl.   Acad.   Sci.   U.   S.   A.*   **2020**,   *117*   (1),   371–380. https://doi.org/10.1073/PNAS.1901493116/SUPPL_FILE/PNAS.1901493116.SD07.XLS X.

(49)   Sofia, H. J.; Chen, G.; Hetzler, B. G.; Reyes-Spindola, J. F.; Miller, N. E.Radical SAM, a Novel Protein Superfamily Linking Unresolved Steps in Familiar Biosynthetic Pathways with Radical Mechanisms: Functional Characterization Using New Analysis and Information Visualization Methods. *Nucleic Acids Res.* **2001**, *29* (5), 1097. https://doi.org/10.1093/NAR/29.5.1097.

(50)   Joan B., B.; Benjamin R., D.; Kaitlin S., D.; Eric M., S.Radical S-Adenosylmethionine Enzymes. *Chem. Rev.* **2014**, *114*, 4229–4317. https://doi.org/10.1021/cr4004709.

(51)   Grell, T. A. J.; Bell, B. N.; Nguyen, C.; Dowling, D. P.; Bruender, N. A.; Bandarian, V.; Drennan, C. L.Crystal Structure of AdoMet Radical Enzyme 7-Carboxy-7-Deazaguanine Synthase from Escherichia Coli Suggests How Modifications near [4Fe–4S] Cluster Engender Flavodoxin Specificity. *Protein Sci.* **2019**, *28* (1), 202–215. https://doi.org/10.1002/PRO.3529.

(52)   Haft, D. H.Bioinformatic Evidence for a Widely Distributed, Ribosomally Produced Electron Carrier Precursor, Its Maturation Proteins, and Its Nicotinoprotein Redox Partners. *BMC Genomics* **2011**, *12* (1), 1–14. https://doi.org/10.1186/1471-2164-12-21/FIGURES/5.

(53)   Haft, D. H.; Basu, M. K.Biological Systems Discovery in Silico: Radical S-Adenosylmethionine Protein Families and Their Target Peptides for Posttranslational Modification. *J. Bacteriol.* **2011**, *193* (11), 2745–2755. https://doi.org/10.1128/JB.00040-11.

(54)   Haft, D. H.; Selengut, J. D.; Richter, R. A.; Harkins, D.; Basu, M. K.; Beck, E.TIGRFAMs and Genome Properties in 2013. *Nucleic Acids Res.* **2013**, *41* (D1), 387–395. https://doi.org/10.1093/nar/gks1234.

(55)   Ruszczycky, M. W.; Zhong, A.; Liu, H. wen.Following the Electrons: Peculiarities in the Catalytic Cycles of Radical SAM Enzymes. *Nat. Prod. Rep.* **2018**, *35* (7), 615. https://doi.org/10.1039/C7NP00058H.

(56)   Ayikpoe, R.; Ngendahimana, T.; Langton, M.; Bonitatibus, S.; Walker, L. M.; Eaton, S. S.; Eaton, G. R.; Pandelia, M. E.; Elliott, S. J.; Latham, J. A.Spectroscopic and Electrochemical Characterization of the Mycofactocin Biosynthetic Protein, MftC, Provides Insight into Its Redox Flipping Mechanism. *Biohcemistry* **2019**, *58*, 940–950.

(57)   Barr, I.; Latham, J. A.; Iavarone, A. T.; Chantarojsiri, T.; Hwang, J. D.; Klinman, J. P.Demonstration That the Radical S-Adenosylmethionine (SAM) Enzyme PqqE Catalyzes de Novo Carbon-Carbon Cross-Linking within a Peptide Substrate PqqA in the Presence of the Peptide Chaperone PqqD. *J. Biol. Chem.* **2016**, *291* (17), 8877–8884. https://doi.org/10.1074/jbc.C115.699918.

(58)   Benjdia, A.; Decamps, L.; Guillot, A.; Kubiak, X.; Ruffié, P.; Sandström, C.; Berteau, O.Insights into the Catalysis of a Lysine-Tryptophan Bond in Bacterial Peptides by a SPASM Domain Radical S-Adenosylmethionine (SAM) Peptide Cyclase. *J. Biol. Chem.* **2017**, *292* (26), 10835–10844. https://doi.org/10.1074/jbc.M117.783464.

(59)   Caruso, A.; Bushin, L. B.; Clark, K. A.; Martinie, R. J.; Seyedsayamdost, M. R.Radical Approach to Enzymatic β-Thioether Bond Formation. *J. Am. Chem. Soc.* **2018**, *141* (2), 990–997. https://doi.org/10.1021/JACS.8B11060.

(60)   Bruender, N. A.; Wilcoxen, J.; Britt, R. D.; Bandarian, V.Biochemical and Spectroscopic Characterization of a Radical SAM Enzyme Involved in the Formation of a Peptide Thioether Crosslink. *Biochemistry* **2016**, *55* (14), 2122–2134. https://doi.org/10.1021/acs.biochem.6b00145.

(61)   Flühe, L.; Burghaus, O.; Wieckowski, B. M.; Giessen, T. W.; Linne, U.; Marahiel, M. a.Two [4Fe-4S] Clusters Containing Radical SAM Enzyme SkfB Catalyze Thioether Bond Formation during the Maturation of the Sporulation Killing Factor. *J. Am. Chem. Soc.* **2013**, *135* (3), 959–962. https://doi.org/10.1021/ja310542g.

(62)   Wieckowski, B. M.; Hegemann, J. D.; Mielcarek, A.; Boss, L.; Burghaus, O.; Marahiel, M. A.The PqqD Homologous Domain of the Radical SAM Enzyme ThnB Is Required for Thioether Bond Formation during Thurincin H Maturation. *FEBS Lett.* **2015**, *589* (15), 1802–1806. https://doi.org/10.1016/j.febslet.2015.05.032.

(63)   Daniel H., H.; Malay Kumar, B.Biological Systems Discovery In Silico: Radical S-Adenosylmethionine Protein Families and Their Target Peptides for Posttranslational Modification. *J. Bacteriol.* **2011**, *193*, 2745–2755. https://doi.org/10.1128/JB.00040-11.

(64)   Kenzie A., C.; Leah B., B.; Mohammad R., S.Aliphatic Ether Bond Formation Expands the Scope of Radical SAM Enzymes in Natural Product Biosynthesis. *J. Am. Chem. Soc.* **2019**, *141*, 10610–10615. https://doi.org/10.1021/jacs.9b05151.

(65)   Shang, Z.; Winter, J. M.; Kauffman, C. A.; Yang, I.; Fenical, W.Salinipeptins: Integrated Genomic and Chemical Approaches Reveal Unusual d -Amino Acid-Containing Ribosomally Synthesized and Post-Translationally Modified Peptides (RiPPs) from a Great Salt Lake Streptomyces Sp. *ACS Chem. Biol.* **2019**, *14* (3), 415–425. https://doi.org/10.1021/acschembio.8b01058.

(66)   Morinaka, B. I.; Vagstad, A. L.; Helf, M. J.; Gugger, M.; Kegler, C.; Freeman, M. F.; Bode, H. B.; Piel, J.Radical S-Adenosyl Methionine Epimerases: Regioselective Introduction of Diverse D -Amino Acid Patterns into Peptide Natural Products. *Angew. Chemie - Int. Ed.* **2014**, *53* (32), 8503–8507. https://doi.org/10.1002/anie.201400478.

(67)   Bhandari, D. M.; Fedoseyenko, D.; Begley, T. P.Tryptophan Lyase (NosL): A Cornucopia of 5′-Deoxyadenosyl Radical Mediated Transformations. *J. Am. Chem. Soc.* **2016**, *138* (50), 16184–16187. https://doi.org/10.1021/jacs.6b06139.

(68)   Mahanta, N.; Zhang, Z.; Hudson, G. A.; Van DerDonk, W. A.; Mitchell, D. A.Reconstitution and Substrate Specificity of the Radical S-Adenosyl-Methionine

Thiazole C-Methyltransferase in Thiomuracin Biosynthesis. *J. Am. Chem. Soc.* **2017**, *139* (12), 4310–4313. https://doi.org/10.1021/jacs.7b00693.

(69)　　Qiu, Y.; Du, Y.; Wang, S.; Zhou, S.; Guo, Y.; Liu, W.Radical S-Adenosylmethionine Protein NosN Forms the Side Ring System of Nosiheptide by Functionalizing the Polythiazolyl Peptide S-Conjugated Indolic Moiety. *Org. Lett.* **2019**, *21*, 1502–1505. https://doi.org/10.1021/acs.orglett.9b00293.

(70)　　Parent, A.; Guillot, A.; Benjdia, A.; Chartier, G.; Leprince, J.; Berteau, O.The B12-Radical SAM Enzyme PoyC Catalyzes Valine Cβ-Methylation during Polytheonamide Biosynthesis. *J. Am. Chem. Soc.* **2016**, *138* (48), 15515–15518. https://doi.org/10.1021/jacs.6b06697.

(71)　　Ibrahim, M.; Guillot, A.; Wessner, F.; Algaron, F.; Besset, C.; Courtin, P.; Gardan, R.; Monnet, V.Control of the Transcription of a Short Gene Encoding a Cyclic Peptide in Streptococcus Thermophilus: A New Quorum-Sensing System? *J. Bacteriol.* **2007**, *189* (24), 8844–8854. https://doi.org/10.1128/JB.01057-07.

(72)　　M, I.; A, G.; F, W.; F, A.; C, B.; P, C.; R, G.; V, M.Control of the Transcription of a Short Gene Encoding a Cyclic Peptide in Streptococcus Thermophilus: A New Quorum-Sensing System? *J. Bacteriol.* **2007**, *189* (24), 8845–8854. https://doi.org/10.1128/JB.01057-07.

(73)　　Davis, K. M.; Schramma, K. R.; Hansen, W. A.; Bacik, J. P.; Khare, S. D.; Seyedsayamdost, M. R.; Ando, N.Structures of the Peptide-Modifying Radical SAM Enzyme SuiB Elucidate the Basis of Substrate Recognition. *Proc. Natl. Acad. Sci. U. S. A.* **2017**, *114* (39), 10420–10425. https://doi.org/10.1073/pnas.1703663114.

(74)　　Nguyen, T. Q. N.; Tooh, Y. W.; Sugiyama, R.; Nguyen, T. P. D.; Purushothaman, M.; Leow, L. C.; Hanif, K.; Yong, R. H. S.; Agatha, I.; Winnerdy, F. R.; Gugger, M.; Phan, A. T.; Morinaka, B. I.Post-Translational Formation of Strained Cyclophanes in Bacteria. *Nat. Chem. 2020 1211* **2020**, *12* (11), 1042–1053. https://doi.org/10.1038/s41557-020-0519-z.

(75)　　Ma, S.; Chen, H.; Li, H.; Ji, X.; Deng, Z.; Ding, W.; Zhang, Q.Post-Translational Formation of Aminomalonate by a Promiscuous Peptide-Modifying Radical SAM Enzyme. *Angew. Chemie - Int. Ed.* **2021**, *60* (36), 19957–19964. https://doi.org/10.1002/ANIE.202107192.

(76)　　Leah B., B.; Kenzie A., C.; István, P.; Mohammad R., S.Charting an Unexplored Streptococcal Biosynthetic Landscape Reveals a Unique Peptide Cyclization Motif. *J. Am. Chem. Soc.* **2018**, *140*, 17674–17684. https://doi.org/10.1021/jacs.8b10266.

(77)   Caruso, A.; Martinie, R. J.; Bushin, L. B.; Seyedsayamdost, M. R.Macrocyclization via an Arginine-Tyrosine Crosslink Broadens the Reaction Scope of Radical S-Adenosylmethionine Enzymes. *J. Am. Chem. Soc.* **2019**, *141* (42), 16610–16614. https://doi.org/10.1021/JACS.9B09210/ASSET/IMAGES/LARGE/JA9B09210_0004.JPEG.

(78)   Murphy, K.; O'Sullivan, O.; Rea, M. C.; Cotter, P. D.; Ross, R. P.; Hill, C.Genome Mining for Radical SAM Protein Determinants Reveals Multiple Sactibiotic-Like Gene Clusters. *PLoS One* **2011**, *6* (7), 20852. https://doi.org/10.1371/JOURNAL.PONE.0020852.

(79)   Flühe, L.; Burghaus, O.; Wieckowski, B. M.; Giessen, T. W.; Linne, U.; Marahiel, M. A.Two [4Fe-4S] Clusters Containing Radical SAM Enzyme SkfB Catalyze Thioether Bond Formation during the Maturation of the Sporulation Killing Factor. *J. Am. Chem. Soc.* **2013**, *135* (3), 959–962. https://doi.org/10.1021/JA310542G.

(80)   Rea, M. C.; Sit, C. S.; Clayton, E.; O'Connor, P. M.; Whittal, R. M.; Zheng, J.; Vederas, J. C.; Ross, R. P.; Hill, C.Thuricin CD, a Posttranslationally Modified Bacteriocin with a Narrow Spectrum of Activity against Clostridium Difficile. *Proc. Natl. Acad. Sci. U. S. A.* **2010**, *107* (20). https://doi.org/10.1073/pnas.0913554107.

(81)   Mo, T.; Ji, X.; Yuan, W.; Mandalapu, D.; Wang, F.; Zhong, Y.; Li, F.; Chen, Q.; Ding, W.; Deng, Z.; Yu, S.; Zhang, Q.Thuricin Z: A Narrow-Spectrum Sactibiotic That Targets the Cell Membrane. *Angew. Chemie - Int. Ed.* **2019**, *58* (52). https://doi.org/10.1002/anie.201908490.

(82)   Balty, C.; Guillot, A.; Fradale, L.; Brewee, C.; Boulay, M.; Kubiak, X.; Benjdia, A.; Berteau, O.Ruminococcin C, an Anti-Clostridial Sactipeptide Produced by a Prominent Member of the Human Microbiota Ruminococcus Gnavus. *J. Biol. Chem.* **2019**, *294* (40). https://doi.org/10.1074/jbc.RA119.009416.

(83)   Bruender, N. A.; Wilcoxen, J.; Britt, R. D.; Bandarian, V.Biochemical and Spectroscopic Characterization of a Radical S-Adenosyl-l-Methionine Enzyme Involved in the Formation of a Peptide Thioether Cross-Link. *Biochemistry* **2016**, *55* (14), 2122–2134. https://doi.org/10.1021/ACS.BIOCHEM.6B00145.

(84)   Bushin, L. B.; Covington, B. C.; Rued, B. E.; Federle, M. J.; Seyedsayamdost, M. R.Discovery and Biosynthesis of Streptosactin, a Sactipeptide with an Alternative Topology Encoded by Commensal Bacteria in the Human Microbiome. *J. Am. Chem. Soc.* **2020**, *142* (38). https://doi.org/10.1021/jacs.0c05546.

(85)   Nakai, T.; Ito, H.; Kobayashi, K.; Takahashi, Y.; Hori, H.; Tsubaki, M.; Tanizawa, K.; Okajima, T.The Radical S-Adenosyl-L-Methionine Enzyme QhpD

Catalyzes Sequential Formation of Intra-Protein Sulfur-to-Methylene Carbon Thioether Bonds. *J. Biol. Chem.* **2015**, *290* (17), 11144–11166. https://doi.org/10.1074/jbc.M115.638320.

(86)   Ian, B.; Troy A., S.; Anthony S., G.; Tyler L., G.; Jeffrey B., B.; John A., L.; Tyler, C.; Carrie M., W.; R. David, B.; Steven C., A.; Judith P., K.X-Ray and EPR Characterization of the Auxiliary Fe-S Clusters in the Radical SAM Enzyme PqqE. *Biochemistry* **2018**, *57*, 1306–1315. https://doi.org/10.1021/acs.biochem.7b01097.

(87)   B, K.; R, A.; M, T.; JA, L.Mechanistic Elucidation of the Mycofactocin-Biosynthetic Radical S-Adenosylmethionine Protein, MftC. *J. Biol. Chem.* **2017**, *292* (31), 13022–13033. https://doi.org/10.1074/JBC.M117.795682.

(88)   Bulat, K.; Priyanka, A.; Michael, B.; Gareth R., E.; Sandra S., E.; John A., L.Mycofactocin Biosynthesis: Modification of the Peptide MftA by the Radical S-Adenosylmethionine Protein MftC. *FEBS Lett.* *590*, 2538–2548. https://doi.org/10.1002/1873-3468.12249.

(89)   Bruender, N. A.; Bandarian, V.The Radical S -Adenosyl- L-Methionine Enzyme MftC Catalyzes an Oxidative Decarboxylation of the C-Terminus of the MftA Peptide. *Biochemistry* **2016**, *55* (20), 2813–2816. https://doi.org/10.1021/acs.biochem.6b00355.

(90)   Macrocyclization via an Arginine-Tyrosine Crosslink Broadens the Reaction Scope of Radical S-Adenosylmethionine Enzymes | Journal of the American Chemical Society. September 5, 2021.

(91)   Nguyen, T. Q. N.; Tooh, Y. W.; Sugiyama, R.; Nguyen, T. P. D.; Purushothaman, M.; Leow, L. C.; Hanif, K.; Yong, R. H. S.; Agatha, I.; Winnerdy, F. R.; Gugger, M.; Phan, A. T.; Morinaka, B. I.Post-Translational Formation of Strained Cyclophanes in Bacteria. *Nat. Chem.* **2020**, *12* (11), 1042–1053. https://doi.org/10.1038/s41557-020-0519-z.

(92)   Kostenko, A.; Lien, Y.; Mendauletova, A.; Ngendahimana, T.; Novitskiy, I. M.; Eaton, S. S.; Latham, J. A.Identification of a Poly-Cyclopropylglycine-Containing Peptide via Bioinformatic Mapping of Radical S-Adenosylmethionine Enzymes. *J. Biol. Chem.* **2022**, 101881. https://doi.org/10.1016/j.jbc.2022.101881.

(93)   Benjdia, A.; Decamps, L.; Guillot, A.; Kubiak, X.; Ruffie, P.; Sandstrom, C.; Berteau, O.Insights into Catalysis of Lysine-Tryptophan Bond in Bacterial Peptides by a SPASM-Domain Radical SAM Peptide Cyclase. *J. Biol. Chem.* **2017**. https://doi.org/10.1074/jbc.M117.783464.

(94)   Leif, F.; Thomas A., K.; Michael J., G.; Antje, S.; Olaf, B.; Uwe, L.; Mohamed A., M.The Radical SAM Enzyme AlbA Catalyzes Thioether Bond Formation in Subtilosin A. *Nat. Chem. Biol.* **2012**, *8*, 350–357. https://doi.org/10.1038/nchembio.798.

(95)   Tyler L., G.; Paul M., H.; Sungwon, H.; Hayretin, Y.; Jeffrey B., B.; Brian, K.; Steven C., A.; Albert A., B.Structural Insights into Thioether Bond Formation in the Biosynthesis of Sactipeptides. *J. Am. Chem. Soc.* **2017**, *139*, 11734–11744. https://doi.org/10.1021/jacs.7b01283.

(96)   Bruender, N. A.; Wilcoxen, J.; Britt, R. D.; Bandarian, V.Biochemical and Spectroscopic Characterization of a Radical S-Adenosyl-L-Methionine Enzyme Involved in the Formation of a Peptide Thioether Cross-Link. *Biochemistry* **2016**, *55* (14), 2122–2134. https://doi.org/10.1021/acs.biochem.6b00145.

(97)   Tadashi, N.; Hiroto, I.; Kazuo, K.; Yasuhiro, T.; Hiroshi, H.; Motonari, T.; Katsuyuki, T.; Toshihide, O.The Radical S-Adenosyl-L-Methionine Enzyme QhpD Catalyzes Sequential Formation of Intra-Protein Sulfur-to-Methylene Carbon Thioether Bonds. *J. Biol. Chem.* **2015**, *290*, 11144–11166. https://doi.org/10.1074/jbc.M115.638320.

(98)   Caruso, A.; Seyedsayamdost, M. R.Radical SAM Enzyme QmpB Installs Two 9-Membered Ring Sactionine Macrocycles during Biogenesis of a Ribosomal Peptide Natural Product. *J. Org. Chem.* **2021**, *86* (16), 11284–11289. https://doi.org/10.1021/acs.joc.1c01507.

(99)   Caruso, A.; Bushin, L. B.; Clark, K. A.; Martinie, R. J.; Seyedsayamdost, M. R.Radical Approach to Enzymatic β-Thioether Bond Formation. *J. Am. Chem. Soc.* **2019**, *141* (2), 990–997. https://doi.org/10.1021/jacs.8b11060.

(100)   Hudson, G. A.; Burkhart, B. J.; DiCaprio, A. J.; Schwalen, C. J.; Kille, B.; Pogorelov, T.V.; Mitchell, D. A. Bioinformatic Mapping of Radical S - Adenosylmethionine-Dependent Ribosomally Synthesized and Post-Translationally Modified Peptides Identifies New Cα, Cβ, and Cγ-Linked Thioether-Containing Peptides . *J. Am. Chem. Soc.* **2019**, *141*, 8228–8238. https://doi.org/10.1021/jacs.9b01519.

(101)   Timothy W., P.; Nilkamal, M.; Douglas A., M.Reconstitution and Substrate Specificity of the Thioether-Forming Radical S-Adenosylmethionine Enzyme in Freyrasin Biosynthesis. *ACS Chem. Biol.* **2019**, *14*, 1981–1989. https://doi.org/10.1021/acschembio.9b00457.

(102)   Clark, K. A.; Bushin, L. B.; Seyedsayamdost, M. R.Aliphatic Ether Bond Formation Expands the Scope of Radical SAM Enzymes in Natural Product Biosynthesis. *J. Am. Chem. Soc.* **2019**, *141* (27), 10610–10615. https://doi.org/10.1021/jacs.9b05151.

(103)   Morinaka, B. I.; Lakis, E.; Verest, M.; Helf, M. J.; Scalvenzi, T.; Vagstad, A. L.; Sims, J.; Sunagawa, S.; Gugger, M.; Piel, J.Natural Noncanonical Protein Splicing Yields Products with Diverse β-Amino Acid Residues. *Science* **2018**, *359* (6377), 779–782. https://doi.org/10.1126/SCIENCE.AAO0157.

(104)   Bruender, N. A.; Wilcoxen, J.; Britt, R. D.; Bandarian, V.Biochemical and Spectroscopic Characterization of a Radical S-Adenosyl- l -Methionine Enzyme Involved in the Formation of a Peptide Thioether Cross-Link. *Biochemistry* **2016**, *55* (14), 2122–2134. https://doi.org/10.1021/ACS.BIOCHEM.6B00145/ASSET/IMAGES/LARGE/BI-2016-00145B_0008.JPEG.

(105)   Mendauletova, A.; Kostenko, A.; Lien, Y.; Latham, J.How a Subfamily of Radical S-Adenosylmethionine Enzymes Became a Mainstay of Ribosomally Synthesized and Post-Translationally Modified Peptide Discovery. *ACS Bio Med Chem Au* **2021**, *2* (1), 53–59. https://doi.org/10.1021/ACSBIOMEDCHEMAU.1C00045.

(106)   Kostenko, A.; Lien, Y.; Mendauletova, A.; Ngendahimana, T.; Novitskiy, I. M.; Eaton, S. S.; Latham, J. A.Identification of a Poly-Cyclopropylglycine–Containing Peptide via Bioinformatic Mapping of Radical S-Adenosylmethionine Enzymes. *J. Biol. Chem.* **2022**, *298* (5), 101881. https://doi.org/10.1016/J.JBC.2022.101881.

(107)   Bulat, K.; Richard, A.; Mason, T.; John A., L.Mechanistic Elucidation of the Mycofactocin-Biosynthetic Radical S-Adenosylmethionine Protein, MftC. *J. Biol. Chem.* **2017**, *292*, 13022–13033. https://doi.org/10.1074/jbc.M117.795682.

(108)   Oberg, N.; Precord, T. W.; Mitchell, D. A.; Gerlt, J. A.RadicalSAM.Org: A Resource to Interpret Sequence-Function Space and Discover New Radical SAM Enzyme Chemistry. *ACS Bio Med Chem Au* **2022**, *2* (1), 22–35. https://doi.org/10.1021/acsbiomedchemau.1c00048.

(109)   Zallot, R.; Oberg, N.; Gerlt, J. A.The EFI Web Resource for Genomic Enzymology Tools: Leveraging Protein, Genome, and Metagenome Databases to Discover Novel Enzymes and Metabolic Pathways. *Biochemistry* **2019**, *58* (41), 4169–4182. https://doi.org/10.1021/acs.biochem.9b00735.

(110)   Layer, G.; Heinz, D. W.; Jahn, D.; Schubert, W. D.Structure and Function of Radical SAM Enzymes. *Curr. Opin. Chem. Biol.* **2004**, *8* (5), 468–476. https://doi.org/10.1016/J.CBPA.2004.08.001.

(111)   Goldman, P. J.; Grove, T. L.; Sites, L. a; McLaughlin, M. I.; Booker, S. J.; Drennan, C. L.X-Ray Structure of an AdoMet Radical Activase Reveals an Anaerobic Solution for Formylglycine Posttranslational Modification. *Proc. Natl. Acad. Sci. U. S. A.* **2013**, *110* (21), 8519–8524. https://doi.org/10.1073/pnas.1302417110.

(112)   Gerlt, J. A.; Bouvier, J. T.; Davidson, D. B.; Imker, H. J.; Sadkhin, B.; Slater, D. R.; Whalen, K. L.Enzyme Function Initiative-Enzyme Similarity Tool (EFI-EST): A Web Tool for Generating Protein Sequence Similarity Networks. *Biochim. Biophys. Acta -*

Proteins Proteomics **2015**, *1854* (8), 1019–1037. https://doi.org/10.1016/j.bbapap.2015.04.015.

APPENDIX A

List of Publications

Kostenko, A., **Lien, Y.**, Mendauletova, A., Ngendahimana, T., Novitskiy, I., Eaton, G.R., Eaton, S.S., and Latham, J.A. Bioinformatic mapping of radical S-adenosylmethionine enzymes yields a unique poly-oxazocanone containing ribosomally synthesized and post-translationally modified peptide. *J. Biol. Chem.* 2022, 298, 5, 101881.

Mendauletova, A., Kostenko, A., **Lien, Y.**, and Latham, J.A. How a subfamily of radical-S-adenosylmethionine proteins became a mainstay of ribosomally synthesized and post-translationally modified peptide discovery. *ACS Bio and Med Chem Au*. 2022, 2, 1, 53-59.

Lien, Y., Zizola, C., Mendauletova, A., Ngendahimana, T., Kostenko, A., Eaton, S.S., Grove, T.L., and Latham, J.A. A new class of cyclopropylsynthases. In preparation.

Table 3. MS ions of starting material (SM) TigB-3R and TigB-3R * products isolated from overnight reaction with TigE. Ions with 2 Da, 4 Da, and 6 Da lighter masses compared to unreacted TigB-3R are consistent with the one, two, and three modifications on the peptide.

	Charge state [2+]			Charge state [3+]		
	Observed m/z	Predicted m/z	Δ ppm	Observed m/z	Predicted m/z	Δ ppm
TigB-3R SM	1627.8739	1627.8526	13.0	1085.5685	1085.5708	-2.1
TigB-3R* 1 modification	1626.8674	1626.8448	13.9	1084.9087	1084.8990	8.9
TigB-3R 2 modifications**	1625.8597	1625.8370	14.0	1084.2415	1084.2271	13.3
TigB-3R* 3 modifications**	1624.8515	1624.8292	13.7	1083.5677	1083.5552	11.6

Table 4. The b- and y- fragment ions of unmodified peptide TigB-3R were detected in HR-MS/MS experiments. [M+2H]$^{2+}$ ion with *m/z* 1627.75 was chosen as precursor ion.

y-ions	Observed *m/z*	Theoretical *m/z*	Δ ppm	b-ions	Observed *m/z*	Theoretical *m/z*	Δ ppm
y_2	162.0851	162.0873	13.8	b_2	302.1103	302.1135	10.8
y_3	261.1539	261.1557	7.1	b_3	415.1941	415.1976	8.5
y_4	348.1851	348.1878	7.7	b_4	514.2627	514.2660	6.4
y_5	405.2071	405.2092	5.2	b_5	677.3246	677.3293	6.9
y_6	518.2883	518.2933	9.7	b_6	805.4206	805.4243	4.6
y_7	619.3387	619.3410	3.8	b_7	902.4702	902.4771	7.7
y_8	676.3577	676.3624	6.9	b_8	1015.5532	1015.5611	7.8
y_9	763.3885	763.3945	7.8	b_9	1102.5826	1102.5932	9.6
y_{10}	862.4522	862.4629	12.4	b_{10}	1159.6073	1159.6146	6.3
y_{11}	949.4837	949.4949	11.8	b_{11}	1260.6532	1260.6623	7.2
y_{12}	1036.5159	1036.5269	10.6	b_{12}	1373.7400	1373.7464	4.6
y_{13}	1135.5890	1135.5953	5.6	b_{13}	1430.7605	1430.7678	5.1
y_{14}	1222.6100	1222.6274	14.3	b_{14}	1517.8019	1517.7999	-1.3
y_{15}	1279.6387	1279.6488	7.9	b_{15}	1616.8574	1616.8683	6.7
y_{16}	1392.7203	1392.7329	9.0	b_{16}	1703.8855	1703.9003	8.7
y_{18}	1550.7955	1550.8020	4.2	b_{17}	1760.9305	1760.9218	-4.9
y_{19}	1637.8231	1637.8341	6.7	b_{18}	1861.9593	1861.9694	5.4
y_{22}	1880.9291	1880.9560	14.3	b_{19}	1975.0392	1975.0535	7.3
y_{26}	2239.1521	2239.1412	-4.9	b_{20}	2032.0513	2032.0750	11.7
y_{28}	2449.2636	2449.2780	5.9	b_{21}	2119.0814	2119.1070	12.1
				b_{22}	2218.1474	2218.1754	12.6
				b_{23}	2305.1764	2305.2074	13.4
				b_{25}	2491.2868	2491.3079	8.5
				b_{26}	2578.3166	2578.3399	9.0
				b_{28}	2906.5076	2906.5146	2.4

Table 5. The b- and y- fragment ions of modified peptide TigB-3R with 2 Da loss were detected in HR-MS/MS experiments. [M+2H]$^{2+}$ ion of TigB-3R* with single modification (*m/z* 1626.75) was chosen as precursor ion. *, fragments with 2 H loss. Fragmentation data for product with modification in the last TIGSVS repeat was used for representation.

y-ions	Observed *m/z*	Theoretical *m/z*	Δ ppm	b-ions	Observed *m/z*	Theoretical *m/z*	Δ ppm
y_2	162.0854	162.0873	11.7	b_2	302.1109	302.1135	8.5
y_4	348.1883	348.1878	-1.5	b_3	415.1932	415.1976	10.7
y_5	405.2080	405.2092	2.9	b_4	514.2614	514.2660	9.0
$y_6{}^*$	516.2731	516.2776	8.8	b_5	677.3244	677.3293	7.2
$y_7{}^*$	617.3211	617.3253	6.8	b_6	805.4176	805.4243	8.3
$y_8{}^*$	674.3457	674.3468	1.6	b_7	902.4729	902.4771	4.6
$y_9{}^*$	761.3737	761.3788	6.7	b_8	1015.5523	1015.5611	8.7
$y_{10}{}^*$	860.4383	860.4472	10.4	b_9	1102.5844	1102.5932	8.0
$y_{11}{}^*$	947.4725	947.4793	7.2	b_{10}	1159.6049	1159.6146	8.4
$y_{12}{}^*$	1034.5042	1034.5113	6.9	b_{11}	1260.6520	1260.6623	8.1
$y_{15}{}^*$	1277.6308	1277.6332	1.9	b_{12}	1373.7299	1373.7464	12.0
$y_{16}{}^*$	1390.7030	1390.7172	10.2	b_{13}	1430.7593	1430.7678	5.9
$y_{18}{}^*$	1548.7656	1548.7864	13.4	b_{14}	1517.7946	1517.7999	3.5
$y_{19}{}^*$	1635.7829	1635.8184	21.7	b_{15}	1616.8228	1616.8683	28.2
$y_{21}{}^*$	1821.8784	1821.9189	22.2	b_{16}	1703.8849	1703.9003	9.1
$y_{22}{}^*$	1878.9423	1878.9403	-1.1	b_{17}	1760.8814	1760.9218	22.9
$y_{26}{}^*$	2237.1103	2237.1256	6.9	b_{18}	1861.9546	1861.9694	7.9
$y_{28}{}^*$	2447.2382	2447.2624	9.9	b_{19}	1975.0361	1975.0535	8.8
				b_{22}	2218.1478	2218.1754	12.4
				b_{23}	2305.2113	2305.2074	-1.7
				b_{25}	2491.2887	2491.3079	7.7

52

Table 6. The b- and y- fragment ions of modified peptide TigB-3R with 4 Da loss were detected in HR-MS/MS experiments. $[M+2H]^{2+}$ ion of TigB-3R with double modification (*m/z* 1625.75) was chosen as precursor ion. [*], fragments with 2 H loss. [**], fragments with 4 H loss. Fragmentation data for product with modification in the first and last TIGSVS repeat were used for representation.

y-ions	Observed *m/z*	Theoretical *m/z*	Δ ppm	b-ions	Observed *m/z*	Theoretical *m/z*	Δ ppm
y_2	162.0854	162.0873	12.0	b_2	302.1105	302.1135	9.9
y_5	405.2057	405.2092	8.7	b_3	415.1939	415.1976	9.0
y_6^*	516.2732	516.2776	8.6	b_4	514.2626	514.2660	6.6
y_7^*	617.3189	617.3253	10.4	b_5	677.3273	677.3293	3.0
y_8^*	674.3413	674.3468	8.2	b_6	805.4189	805.4243	6.8
y_9^*	761.3727	761.3788	8.0	b_7	902.4706	902.4771	7.2
y_{10}^*	860.4439	860.4472	3.8	b_8	1015.5523	1015.5611	8.7
y_{11}^*	947.4755	947.4793	4.0	b_9	1102.5888	1102.5932	4.0
y_{12}^*	1034.5063	1034.5113	4.8	b_{10}	1159.6087	1159.6146	5.1
y_{13}^*	1133.5681	1133.5797	10.2	b_{11}	1260.6565	1260.6623	4.6
y_{14}^*	1220.6110	1220.6117	0.6	b_{12}^*	1371.7239	1371.7307	4.9
y_{15}^*	1277.6240	1277.6332	7.2	b_{13}^*	1428.7490	1428.7522	2.2
y_{16}^*	1390.6883	1390.7172	20.8	b_{14}^*	1515.7723	1515.7842	7.9
y_{18}^*	1548.7757	1548.7864	6.9	b_1^{**}	1614.8457	1614.8526	4.3
y_{19}^*	1635.8157	1635.8184	1.6	b_{16}^*	1701.8732	1701.8846	6.7
y_{21}^*	1821.8704	1821.9189	26.6	b_{17}^*	1758.9055	1758.9061	0.3
y_{22}^*	1878.9410	1878.9403	-0.4	b_{18}^*	1859.9466	1859.9538	3.9
y_{23}^{**}	1989.9811	1990.0087	13.9	b_{19}^*	1973.0163	1973.0379	11.0
y_{28}^{**}	2445.1915	2445.2467	22.6	b_{22}^*	2216.1562	2216.1598	1.6
				b_{25}^*	2489.2639	2489.2922	11.4
				b_{30}^{**}	2902.4179	2902.4833	22.5

Table 7. The b- and y- fragment ions of modified peptide TigB-3R with 6 Da loss were detected in HR-MS/MS experiments. [M+2H]$^{2+}$ ion of TigB-3R with triple modification (m/z 1624.75) was chosen as precursor ion. *, fragments with 2 H loss. **, fragments with 4 H loss. ***, fragments with 6 H loss.

y-ions	Observed m/z	Theoretical m/z	Δ ppm	b-ions	Observed m/z	Theoretical m/z	Δ ppm
y_2	162.0846	162.0873	16.8	b_2	302.1107	302.1135	9.2
y_5	405.2052	405.2092	9.9	b_3	415.1931	415.1976	11.0
y_6^*	516.2727	516.2776	9.5	b_4	514.2609	514.2660	9.8
y_7^*	617.3154	617.3253	16.0	b_5	677.3247	677.3293	6.9
y_8^*	674.3428	674.3468	5.9	b_6	805.4184	805.4243	7.4
y_9^*	761.3719	761.3788	9.0	b_7	902.4776	902.4771	-0.6
y_{10}^*	860.4426	860.4472	5.4	b_8	1015.5534	1015.5611	7.6
y_{11}^*	947.4732	947.4793	6.5	b_9	1102.5861	1102.5932	6.4
y_{12}^*	1034.5023	1034.5113	8.7	b_{10}	1159.6086	1159.6146	5.2
y_{15}^*	1277.6285	1277.6332	3.7	b_{11}	1260.6498	1260.6623	9.9
y_{16}^{**}	1388.6974	1388.7016	3.0	b_{12}^*	1371.7216	1371.7307	6.6
y_{18}^{**}	1546.7618	1546.7707	5.8	b_{13}^*	1428.7453	1428.7522	4.8
y_{19}^{**}	1633.7903	1633.8028	7.7	b_{14}^*	1515.7708	1515.7842	8.9
y_{21}^{**}	1819.8681	1819.9032	19.3	b_{15}^*	1614.8441	1614.8526	5.3
y_{22}^{**}	1876.9169	1876.9247	4.2	b_{16}^*	1701.8720	1701.8846	7.4
y_{23}^{***}	1988.0277	1987.9931	-17.4	b_{17}^*	1758.8941	1758.9061	6.8
				b_{18}^*	1859.9452	1859.9538	4.6
				b_{19}^{**}	1971.0051	1971.0222	8.7
				b_{20}^{**}	2028.0512	2028.0437	-3.7
				b_{22}^{**}	2214.1408	2214.1441	1.5
				b_{25}^{**}	2487.2452	2487.2766	12.6
				b_{30}^{***}	2900.5264	2900.4676	-20.3

Table 8. Sequences of substrate variants used in this study. All the peptides are amidated at C-terminus.

TigB-3R	MDLVYKPISGTIGSVSGTIGSVSSVSGTIGSVSG-Am	up to -6 Da
$^{13}C_5$ ^{15}N Val$_5$ TigB-3R	MDLVYKPISGTIGSVSGTIGSVSSVSGTIGSVSG-Am	up to -6 Da
$^{13}C_6$ ^{15}N Ile$_3$ TigB-3R	MDLVYKPISGTIGSVSGTIGSVSSVSGTIGSVSG-Am	up to -6 Da
(I to A)$_4$ TigB-3R	MDLVYKPASGTAGSVSGTAGSVSSVSGTAGSVSG-Am	no reaction
(I to V)$_3$ TigB-3R	MDLVYKPVSGTVGSVSGTVGSVSSVSGTVGSVSG-Am	-2 Da

Figure 13. ^{13}C HSQC NMR spectra of the substrate peptide TigB-3R and TigE product. **A)** Substrate peptide TigB-3R. **B)** TigE product in deuterated DMSO recorded on Bruker 500 MHz.

A
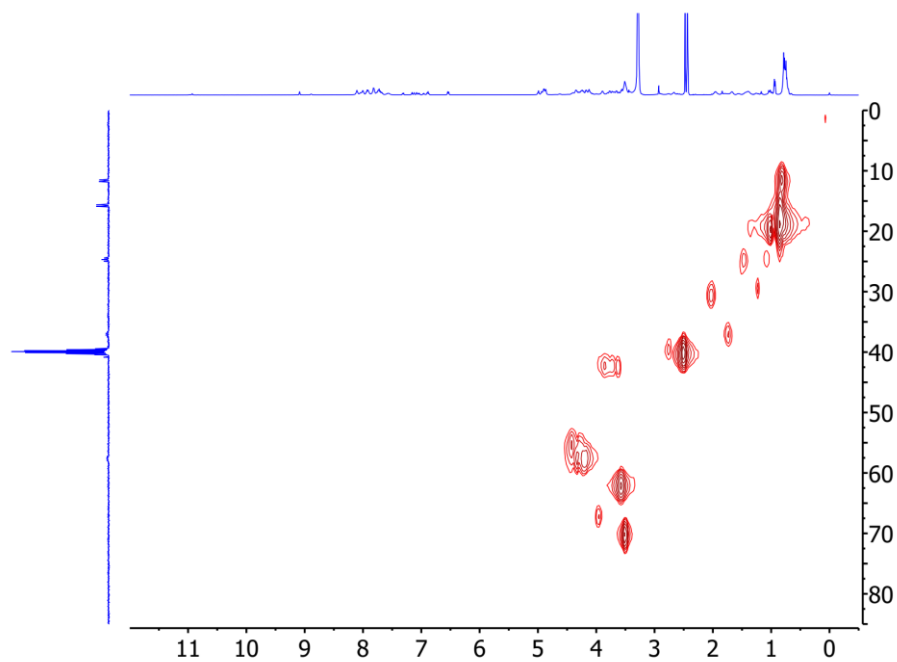
B
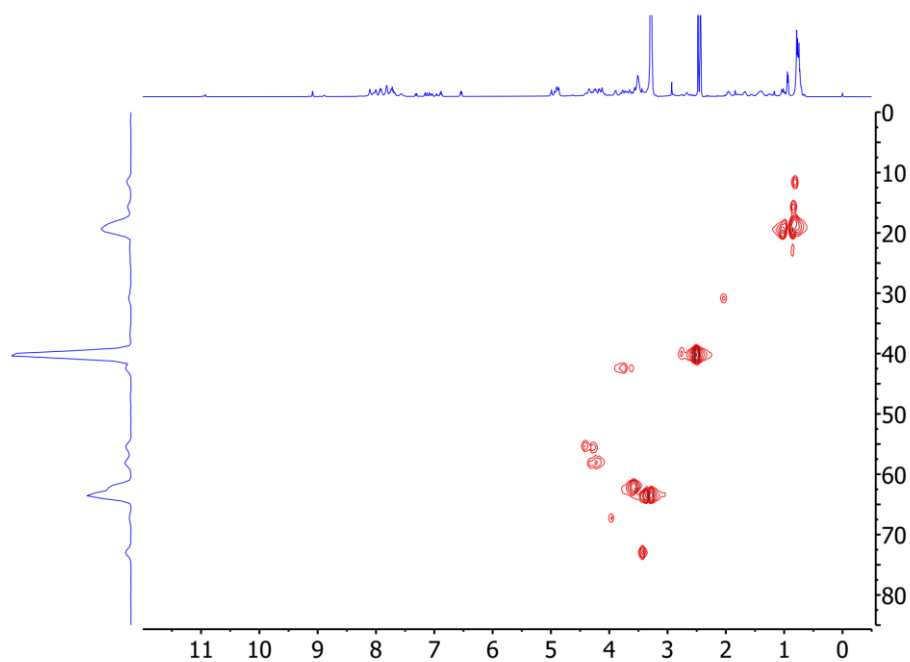
Figure 14. ^{1}H NMR spectra of the substrate peptide TigB-3R and TigE product. **A)** Substrate peptide TigB-3R. **B)** TigE product in deuterated DMSO recorded on Bruker 500 MHz.

A
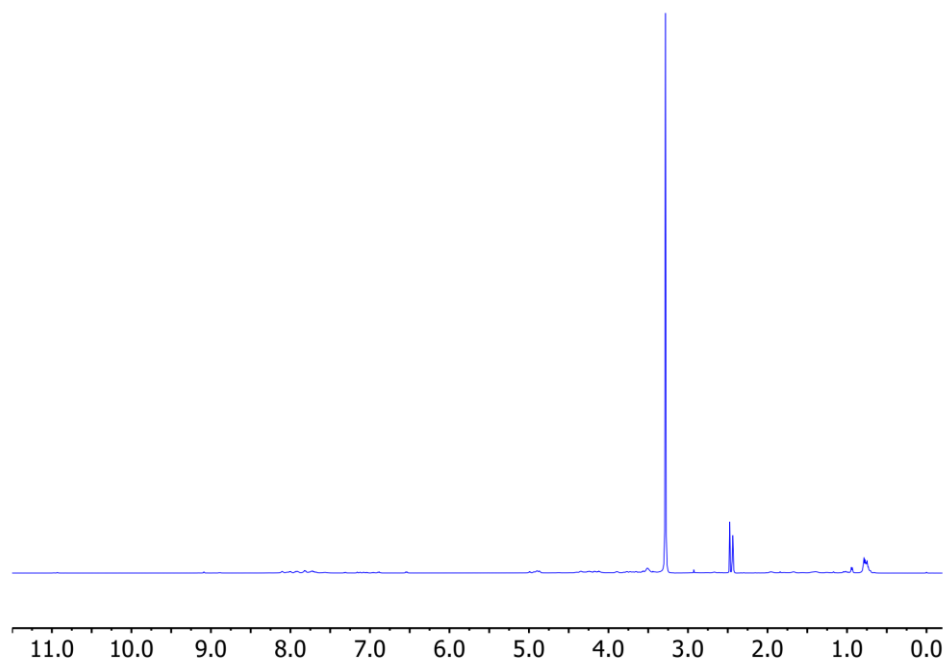
B
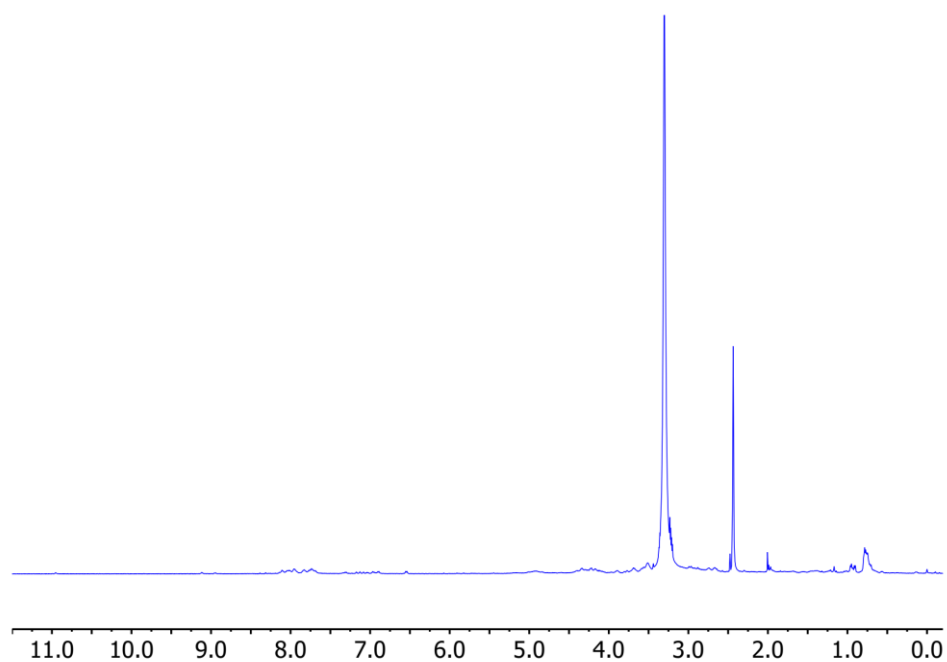
Figure 15. ^{13}C HSQC NMR spectra of the substrate peptide ^{13}C$_6$ ^{15}N Ile$_3$ TigB-3R variant and its modified product. **A)** Substrate peptide ^{13}C$_6$ ^{15}N Ile$_3$ TigB-3R variant. **B)** Modified ^{13}C$_6$ ^{15}N Ile$_3$ TigB-3R variant in deuterated DMSO recorded on Bruker 500 MHz.

A

B
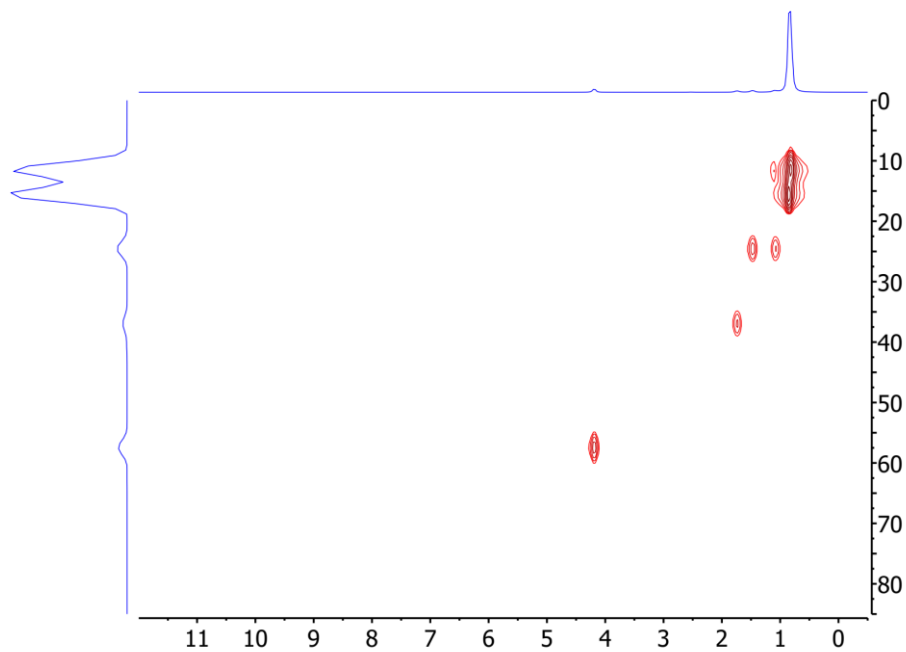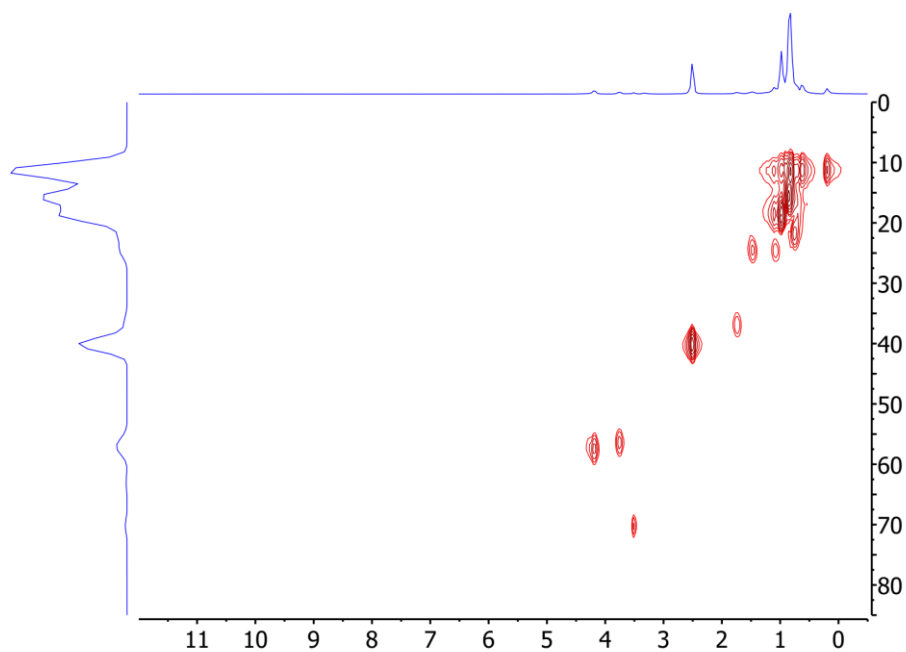
Figure 16. Overlayed ^{13}C HSQC of TigB-3R and $^{13}C_6$ ^{15}N Ile$_3$ TigB-3R variant before and after the reaction with TigE. **A)** Overlayed ^{13}C HSQC of TigB-3R before (green) and after (red) the reaction with TigE recorded in deuterated DMSO on Bruker 500 MHz. **B)** Overlayed ^{13}C HSQC NMR spectra of the unmodified (green) and modified (red) $^{13}C_6$ ^{15}N Ile$_3$ TigB-3R variant recorded in deuterated DMSO on Bruker 500 MHz.

A

B